DELIVERABLE

Mapping and health assessment of grey dune habitat in Barreta Island

Action A2

Project

LIFE Ilhas Barreira

Faro | September | 2020

Mapping and health assessment of grey dune habitat in Barreta Island

Project LIFE Ilhas Barreira

CIMA/UAlg – Centro de Investigação Marinha e Ambiental da Universidade do Algarve

Coordenação do projeto no CIMA/UAlg
Óscar Ferreira (CIMA, UAlg)

Equipa técnica/científica
Lara Talavera, Susana Costas, Óscar Ferreira, Luísa Bon de Sousa, Margarida Ramires, Ana Rita Carrasco

www.lifeilhasbarreira.pt

Table of contents

Summary/Resumo

This report describes the methods and the main results achieved on the analysis of the natural and human factors influencing (1) the multi-decadal evolution and dynamics of Barreta Island and its different geomorphological units, and (2) the spatiotemporal changes in both the cover and health of the vegetation present at the grey dunes in the island. The analyses presented here rely on historical maps and remotely-sensed datasets of different nature: aerial photographs, satellite imagery, orthophotos, LiDAR, Google Earth images, and Unmanned Aerial Systems (UAS) covering a period of 70 years approximately.

Barreta/Deserta Island experienced a growth trend as a consequence of the longshore sediment transport and the presence of human infrastructures and activities (e.g. Faro-Olhão Inlet and the Ancão Inlet relocation), which is expected to continue. The vegetation disturbance in the grey dunes at the island started in 2014 over two distinct areas located at the central region that continued expanded until 2020. The factors causing grey dune degradation were mainly attributed to the settlement of Audouin's Gull (*L. audouinii)* and Yellow-legged Gull (*L. michahellis)* colonies (especially due to trampling and plant physical disturbance induced by Yellow-legged Gull) and to a much minor extent to human occupation. Further research should be focused on better understanding the effect that both the image quality and indirect factors have (e.g. seasonal plant shifts, precipitacion, etc.) on the vegetation classification and associated changes.

The approach presented here will allow the definition of adequate conservation measures to be implemented at the barrier that will ensure the protection of the grey dunes and associated species. Furthermore, it can be used in any of the additional 546 locations in which grey dunes are present within the EU Natura 2000 network that could face similar degradation problems.

Este relatório descreve os métodos e os resultados obtidos relativos à análise da influência de fatores antrópicos e naturais na (1) evolução e dinâmica da Illha Barreta e das suas diferentes unidades geomorfológicas, à escala das décadas, e nas (2) variações espaço-temporais no coberto vegetal das dunas cinzentas e do seu estado de conservação. A análise apresentada baseia-se num conjunto de mapas históricos e de dados de deteção remota de fontes diversas: fotografias aéreas, imagens de satelite, ortofotos, LIDAR, imagens do Google Earth e de sistemas aéreos não-tripulados (UAS), abrangendo um período de aproximadamente 70 anos.

A Ilha Barreta (ou Deserta) apresentou uma tendência de crescimento devido ao transporte longilitoral e à presença de infraestruturas e atividades antrópicas (ex. Barra de Faro-Olhão e relocalização da Barra do Ancão). A perturbação da vegetação das dunas cinzentas, nesta ilha, iniciou-se em 2014, em duas áreas distintas, localizadas na zona central da ilha e que possuiram expansão até 2020. Os fatores causadores de degradação dunar são, principalmente, a população de gaivotas, a gaivota-de-audouin (*L. audouinii*) e a gaivota-de-patas-amarelas (*L. michahellis),* sobretudo o pisoteio e a perturbação induzida pela gaivota-de-patas-amarelas) e, numa menor extensão, a ocupação antrópica. Será necessária uma investigação complementar para melhor entender o papel da qualidade das imagens e de fatores indiretos (ex. sazonalidade das plantas, precipitação) na classificação da vegetação e nas suas variações.

A abordagem apresentada permitirá definir medidas de conservação adequadas, a implementar nesta ilha barreira, para proteger as dunas cinzentas e as espécies que lhes estão associadas. Poderá, ainda, ser utilizada em qualquer das 546 áreas em que as dunas cinzentas estão presentes dentro da Rede Natura 2000 e que estejam sujeitas a problemas de degradação similares.

1 | Introduction

In 2008, the Portuguese Marine IBA (Important Bird Area) inventory (published by SPEA), identified a marine IBA at Ria Formosa. The existing baseline information proved to be insufficient, and this IBA never became legally binding. Between 2012 and 2015, Portugal made an important step towards the implementation of the Natura 2000 network in the marine environment, by establishing new marine SPAs (Special Protection Areas). Nevertheless, this process was not aimed towards the conservation of Audouin's Gull (*L. audouinii)*. At the time, the breeding information and distribution data for this species, in Portugal, was considered insufficient. Since then, further work has been developed and new insights indicate that, nowadays, there is a stable meta-population breeding in the uninhabited Barreta Island. Climate change and derived sea-level rise are global-scale problems threatening most of the coastal habitats, among which the barrier islands are not an exception and, as holders of unique ecosystems, they need urgent attention. These islands are also threatened by human pressure and it is urgent to implement measures that can reduce these threats. LIFE Ilhas Barreira aims to characterize the local ecological requirements and conservation threats of the target species and habitats in Ria Formosa, and particularly at Barreta Island, to implement effective conservation actions. This project represents an important step towards the present and future sustainable management of the SPA at Ria Formosa.

1.1 Project objectives

The main project objectives are to:

1. Understand the main threats to the target species (Audouin's Gull and Little Tern *S. albifrons*) and habitats, both on land and at sea;
2. Recover the Grey Dunes habitat and assess the effect of gulls on this habitat;
3. Promote the sustainable use of the Ria Formosa barrier islands and marine area, focusing on fisheries and tourism;
4. Evaluate the effect of climate change and other drivers of change on the eco-morphology of the barrier islands system;
5. Understand the breeding ecology, foraging behaviour and spatial distribution of Audouin's Gull and Little Tern;
6. Evaluate and mitigate bycatch impacts on seabirds and assess the future effect of the discard ban policy on Audouin's Gull local population, engaging the local fisherman community;
7. Evaluate possible competitive interactions and predation from Yellow legged-gull (*L. michahellis)* towards the target species;
8. Protect breeding areas for Audouin's Gull and Little Tern (restricting tourist access, controlling predators, increasing surveillance and implementing environmental awareness campaigns);
9. Review the marine IBA limits and update the marine area of the SPA.

1.2 Deliverable context and objectives within the project

The Action 2 deliverable: ‘’Mapping and health assessment of grey dune habitat in Barreta island’’, was planned to evaluate the conservation state or health of fixed dunes with herbaceous vegetation (i.e. “grey dunes”; priority habitat 2130), contributing to achieve the project objectives 1, 2, 3 and 4. For that, the spatial and temporal distribution of this habitat within Barreta Island was determined to assess the areas with conservation problems, called critical areas. In these areas, further conservation actions must be implemented to ensure their protection and recovery, and this deliverable provides the background information needed to define the conservation measures for actions C1 and C2, at each critical area. The latter will be possible after identifying the causes behind habitat deterioration or disturbance, which will be done also in combination with outputs from action A4, namely by identifying the impact of gulls over the target habitat and assess the impact of human pressure (activities and visitors) over the dunes.

1.3 Approach

The mapping of the grey dunes integrated information from action A1 to define the association of plant species that define this habitat within the islands. The mapping of the dune habitat was based on high-resolution aerial photographs, digital terrain models (DTM) and *in situ* ground-truth surveys. For that, all available aerial photographs and DTMs collected within the frame of previous projects (MICORE, EVREST) were used for habitat mapping through time and space. Available aerial photographs have been orthorectified and georeferenced, covering the period between 1952 and 2014. The period of analysis was extended to the present by downloading Google Earth imagery (2017). Multispectral photographs, namely with the visible and near-infrared radiation bands, were used to produce indexed images showing the actual vegetation cover or leaf health by computing vegetation indexes. The analysis of the aerial photographs also included the mapping of infrastructures or other types of occupation or human interference over the habitat within the island that can be relevant to understand the evolution of the vegetation cover. Two UASs (unmanned aerial systems aka drones) were acquired to make possible a fine evaluation of habitat conservation actions. After testing with the support of ground control points (GCPs) and ground truth surveys, a baseline survey was performed to obtain a cover to be compared with the aerial photographs and to set the reference for the next studies (D1). The above datasets were used to define the typical ranges of vegetation cover within the target grey dune habitat. The obtained results were used to identify disturbance areas by applying an indicator (see Figure 1) resulting from the comparison between optimal values of vegetation density with actual, measured, values. The indicator was spatially and temporally estimated to understand the evolution of the system. The use of this indicator allows informing about disturbed or “un-healthy” habitats regarding the vegetation cover. The latter allows defining the critical or hot spot areas that need protective actions within the study area.

Additionally, this action included the: (i) analysis of the evolution of the shoreline (already characterized within the frame of previous research projects), which will contribute to assessing the relationship between shoreline evolution and the development of new grey dunes; (ii) identification of areas with higher human occupation/pressure; and (iii) spatial distribution of gull breeding areas and associated communities. The latter point had the contribution from outputs from A4.

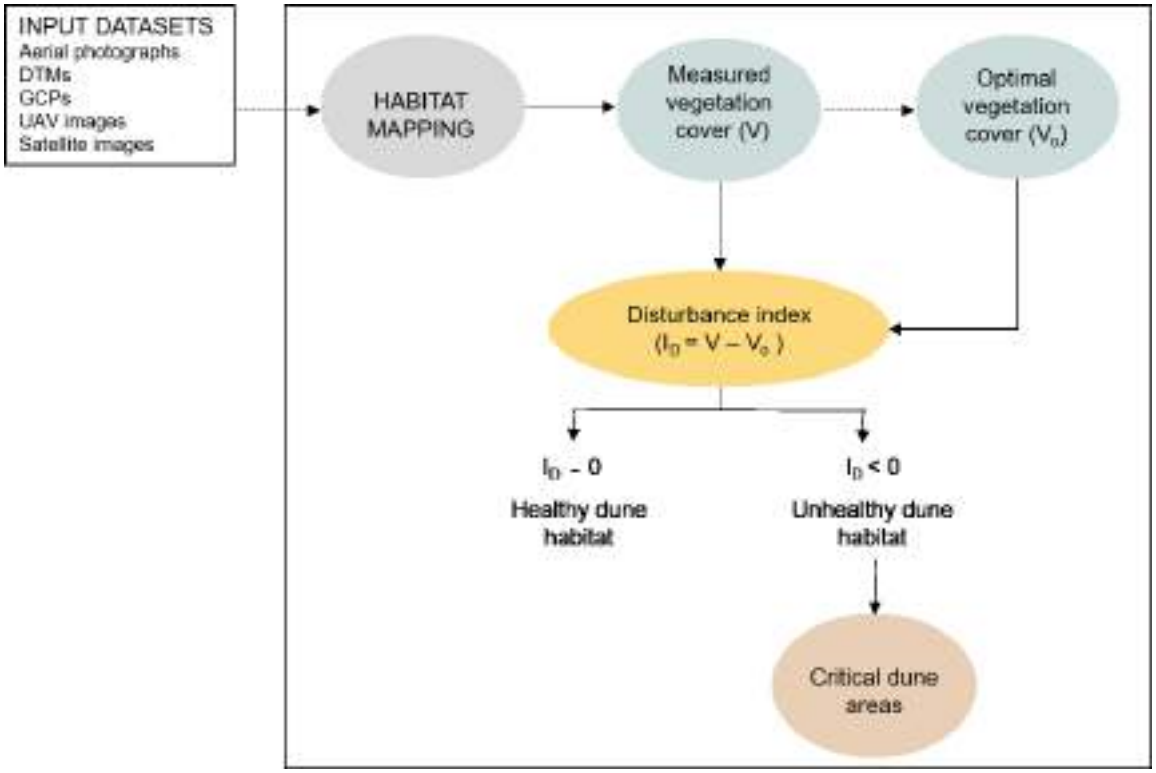

Figure 1 | General workflow.

2 | Objectives of Action 2

This action is planned to evaluate the conservation state or health of the grey dunes (priority habitat 2130) at Ria Formosa, and particularly at Barreta Island, contributing directly or indirectly to achieve the following objectives of the project:

1. Understand the main threats to the target species (Audouin's Gull and Little Tern) and habitats, both on land and at sea;
2. Recover the grey dunes habitat and assess the effect of gulls on this habitat;
3. Promote the sustainable use of the Ria Formosa barrier islands and marine area, focusing on fisheries and tourism;
4. Evaluate the effect of climate change and other drivers of change on the eco-morphology of the barrier islands system.

Additionally, this action will explore the reasons behind the identified disturbed areas in the vegetation cover. The latter point is highly relevant as in recent years a deterioration in the vegetation cover at Barreta Island can be observed that seems to be associated with the settlement of Yellow-legged Gull or other gull species.

3 | Study Area

Barreta Island is one of the seven barriers belonging to the Ria Formosa multi-inlet barrier system, located in South Portugal (Figure 2). This system, declared Natural Park in 1987, is a wetland area comprised by dunes, marshes, and tidal flats of high ecological and socio-economic value. These habitats are protected under the Ramsar convention and included in the list of protected areas within the EU Natura 2000 network.

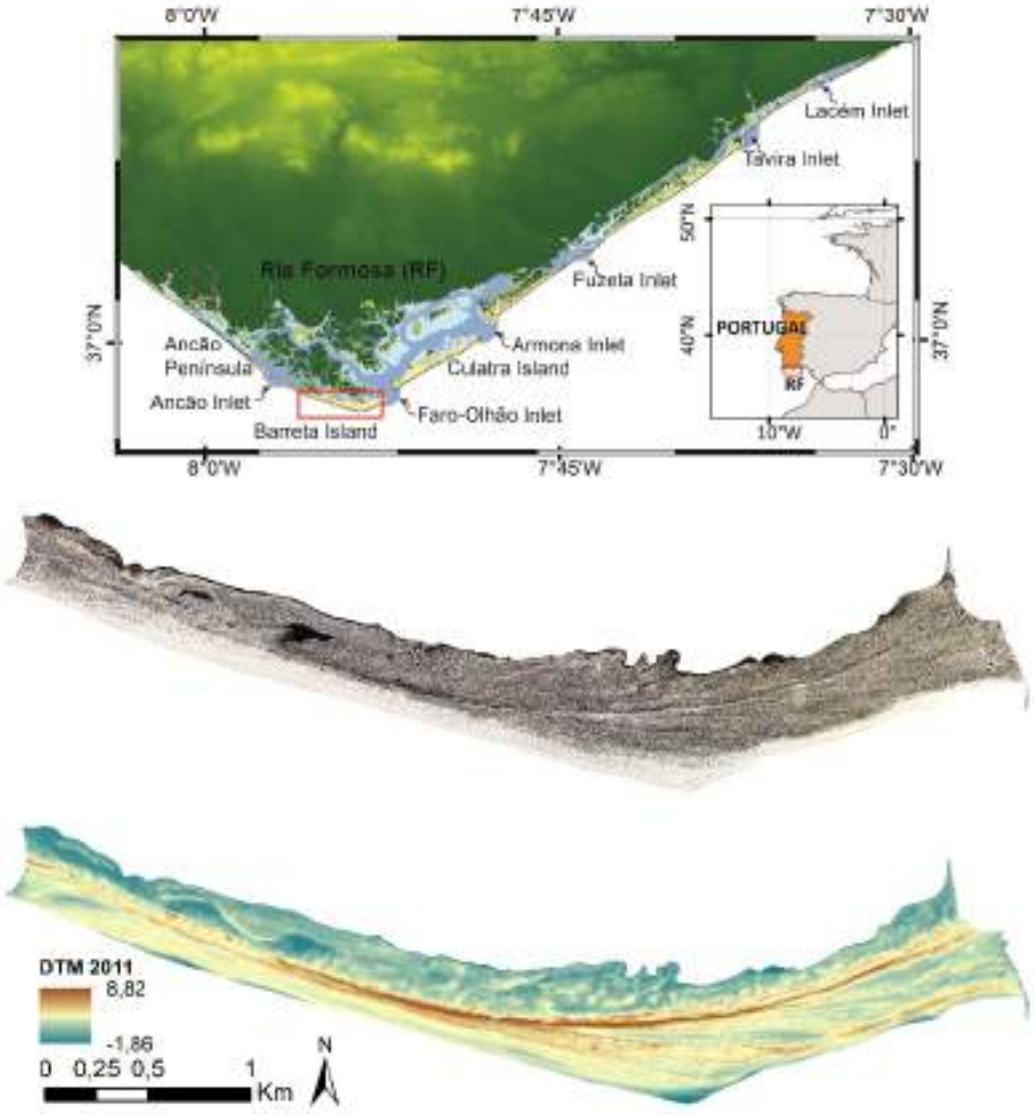

Figure 2 | Barreta Island location (red rectangle) within the Ria Formosa (upper panel), 2014 orthophoto (mid pannel) and 2011 DTM (lower panel).

Ria Formosa is a cuspate-shaped system consisting of five barrier islands and two sandy spits separated by six tidal inlets that connect the lagoon with the Atlantic Ocean. The barrier system is located at a maximum distance of 6 km from the mainland and extends 55 km along an eastern and a western flank. The system's vertex, known as Santa Maria cape, is located in Barreta Island. Waves reach the area from the west-southwest (W-SW) and the east-southeast (E-SE) directions, with 71% and 23% occurrence, respectively (Costa *et al*., 2001). The average annual significant wave height is 0.92 m while the mean annual peak period is 8.2 seconds (Costa *et al*., 2001). This duality in the wave direction is also reflected in the wind regime, which is dominant from the west (W), northwest (NW) and southwest (SW) directions. Eastern winds are more infrequent, although they can be intense and may affect this region, mostly during spring and autumn (Andrade, 1990). The most frequent storms impacting the area come from the W-SW and are associated with low-pressure Atlantic systems typical of the winter, with wave heights up to 7 m. The less frequent E-SE storms are linked to Levante winds originated in the Strait of Gibraltar between October and May, and they generate smaller waves due to the limited fetch (Almeida *et al*., 2011). According to the previous, the western flank of the barrier system concentrates higher wave power than its eastern counterpart (Vila-Concejo *et al*., 2002). The tides in this region are semidiurnal, with neap and spring tides presenting average ranges of 1.3 and 2.8 m, respectively. Maximum spring tidal range can reach up to 3.5 m (Pacheco *et al*., 2008). The main source of sediment in the system comes from the cliffs located up-drift, whose material is eroded and then transported eastwards by the longshore currents (Dias *et al.*, 1992).

The regional climate falls within the Mediterranean hot summer (Csa) Koppen type according to the Portuguese Institute for Sea and Atmosphere, I.P. (IPMA, 2019) which is characterised by a humid (October to April) and a dry season (May to September). In the former, the lowest average temperature is 10º C and the average precipitation values are 50 mm per month, whereas in the second the temperature oscillates between 15 and 25º C, and the precipitation is often close to zero millimetres/month (IPMA, 2019).

Barreta Island is the southernmost island of the system and it is bordered by the Ancão Inlet to the west and the Faro-Olhão Inlet to the east (Figure 3). Both inlets have influenced significantly the morphology of this island. After its first relocation (1996), the Ancão Inlet kept rapidly migrating eastwards and affecting the shore in the western Barreta, which became low and prone to overwash (Matias *et al*., 2008). The new relocation (2015) of the inlet, further to the west, allowed Barreta Island to regain an extension of about 3 km, mostly composed by an unvegetated washover platform. On the other hand, the jetties used to stabilize the Faro-Olhão Inlet induced significant accretion in the eastern part of Barreta due to sediment trapping (Figure 3). Because of these human interventions, from 1952 to 2001 the approximate length of the island had varied from 5,000 m to 9,200 m, and its width increased at the eastward part (Kombiadou *et al*., 2019). A set of different 17 dune ridges have been identified in Barreta Island due to differences in the alongshore response of the island (Herrero *et al*., 2020). Single-ridge dunes with heights lower than 7 m above mean sea level, MSL (Vila-Concejo *et al*., 2006) characterise the western part of the island whereas in the eastern part the dune ridges are high and continuous. Within the dune habitats present in Barreta Island is the 2130 fixed coastal dunes with herbaceous vegetation (also known as 'grey dunes'). According to recent *in situ* observations, the present state of the grey dunes is considered "unfavourable" due to threats derived from tourism, invasive alien species and pressure from *L. michahellis*. Grey dunes are of extreme importance both to maintain the established biodiversity as a shoreline and back-barrier protection against the advances of the sea.

Figure 3 | Drone photo showing the barrier lagoon (left), grey dunes (middle), and beach (right) in the westermost part of Barreta Island.The jetties and the Faro-Olhão inlet appear at the image background.

The beach in Barreta is reflective with a steep beach slope (0.13 to 0.14 at the western part) (Matias *et al*., 2009b), and presents several berms located at an average elevation of 3.2 m, which can reach higher values due to overwash (Matias *et al*., 2009a). The analyses of sediment samples along the foreshore, backshore and foredune at Barreta island showed grain sizes of 746, 497, and 324 µm, respectively (Herrero, 2018).

4 | Shoreline and dune evolution

4.1 Methods

4.1.1 Multi-decadal and short-term coastlines and unit analyses

The analysis of shoreline and dune evolution at Barreta Island consisted on both a multi-decadal and a short-term study of the barrier evolution, including the analysis of shoreline evolution, of its different units (beach, dune and marsh) as well as the examination of the growth mechanisms and geometry of the dune ridges. These analyses were performed using different datasets from 1873 to 2020: historical maps, aerial photos, orthophotos, and Digital Terrain Models (DTMs), all of them georeferenced to the European Terrestrial Reference System 1989 (PT-TM06/ETRS89) (see Table 1). These were obtained from different Portuguese institutions such as the CIGeoE (Centro de Informação Geoespacial do Exército), FAP (Força Aérea Portuguesa), IPCC (Instituto Portugués de Cartografia e Cadastro), DGT (Direção-Geral do Território), and/or CIMA (Centro de Investigação Marinha e Ambiental).

The short- and medium-term evolution of the geomorphological units present at Barreta Island was investigated performing several analyses. The cross-shore coastline evolution rates of the sub-aerial beach, foredune, and back-barrier (in m/yr) were estimated, as also the evolution of both the barrier and dune widths (in m), and the barrier area (in m^2). To do so, different datasets of remotely sensed data were used, namely the historical maps, aerial photos, and orthophotos depicted in Table 1.

Table 1 | Datasets used for the analysis of shoreline and dune evolution (*HM = Historical map, AP = Aerial photograph, O = Orthophoto, Li = LiDAR).

Year	Data	Barrier multi-decadal and short-term analyses	Dune ridge analyses
1873	HM	o	
1885	HM		o
1915	HM	o	
1947	AP	o	o
1952	AP	o	o
1958	AP	o	o
1972	AP	o	o
1976	AP	o	o
1980	AP	o	o
1985	AP	o	o
1986	AP	o	
1989	AP	o	o
1996	AP	o	o
1999	AP	o	o
2000	AP	o	o
2001	AP	o	o
2002	O	o	o
2005	O	o	o
2008	O	o	o
2009	O	o	
2011	Li		o

2014	O	o	o

The cross-shore rates were estimated by digitalising the boundary lines between the different geomorphological units (e.g. the ocean-side coastline, the dune line, the back-barrier coastline in the lagoon side, and the marsh-edge line) in a Geographic Information Sytem (GIS) environment and then applying a Weighted Linear Regression (WLR) using the Digital Shoreline Analysis Tool (DSAS) (Thieler *et al*., 2009). Regarding the barrier and dune widths, these were defined using the same baseline of reference and along evenly spaced transects every 100 m.

The foregoing analyses were correlated with the storms taking place during the past 60 years, as they were considered potential drivers of coastal evolution. These storms were obtained from wave records from the Faro buoy (from 1993 to 2014), as well as hindcasting results (SIMAR; Spanish State Port Authority; Rusu *et al*., 2008) from 1958 to 2014. The reader is referred to the work of Kombiadou *et al.* (2019) for a detailed description of the whole procedure.

4.1.2 Dune ridge analyses: growing mechanisms and geometry

The study of the dune ridge constructive processes in Barreta Island was focused in the high and continuous ridges present along the central region of the island. The reason behind this lies in the fact that it is in this region where the most constant progradation and ridge formation rates were found during the entire period of study. The different analyses performed to investigate ridge growing mechanisms and the parameters influencing their geometry consisted in the individualization of the ridges for dating purposes, and the calculation of ridge accumulation and aggradation rates (in m^3/yr and m/yr, respectively). These ridges are also the habitat for some of the analysed gull species, including *L. audouinii* and *L. michahellis,* being therefore relevant the analysis of their evolution in the context of the evolution of the species breeding and establishment.

The individual ridges were identified from a map of slopes built using the 2011 DTM. The progradation rates were obtained based on a series of coastline positions that were extracted from the 1885 historical map and aerial photos (using the seaward vegetation limit as a proxy), and applying again DSAS. On the other hand, the most likely estimate of ridge formation periods was obtained by comparing the location of each ridge crest to both the vegetation lines and the mean high water level (MHWL), which was also mapped using the abovementioned datasets (see Table 1) and using the debris line or beach scarp as proxies.

The previous ridge formation periods together with the ridge volumes (calculated using the DTM and a baseline of 3.2 m representing the average elevation of the berm crest typical of the winter) allowed the calculation of the accumulation rates (m^3/yr). Lastly, the amount of sediment accumulated vertically within each ridge per year, termed as aggradation rate (in m/yr), was derived dividing the previous accumulation rates (in m^3/yr) by the total ridge area (in m^2).

The metocean conditions influencing the aggradation rates were also examined, namely the annual number of wind events with the potential to initiate aeolian transport, the influence of the number and duration of storm wave events, and the seasonal wave power in the cross-shore and alongshore directions. Moreover, the occurrence of wave run-up levels overtopping the berm was analysed too, and the maximum run-up value was used as a threshold to distinguish the aeolian or marine nature of the constructed ridges. The previous analyses were performed using available hindcasting wind (1960-2007) and wave (1958-2008) data series as well as data from a wave buoy

(continuos series from 1993) located off Santa Maria Cape. Further details regarding the method, parameters, and equations used can be consulted in the work of Herrero *et al*. (2020).

4.2 Results

4.2.1 Multi-decadal and short-term evolution of Barreta Island

Spatio-temporal analyses of the coastlines and environments during the last 60 years showed that strong accretion dominated the sub-aerial beach located up to 6 km west from the jetty. Foredune progradation was fast, showing the highest rates at Santa Maria Cape. Erosion was not significant, although there were some erosive tendencies near the Faro-Olhão Inlet likely derived from local flows formed close to the updrift jetty (Figure 4).

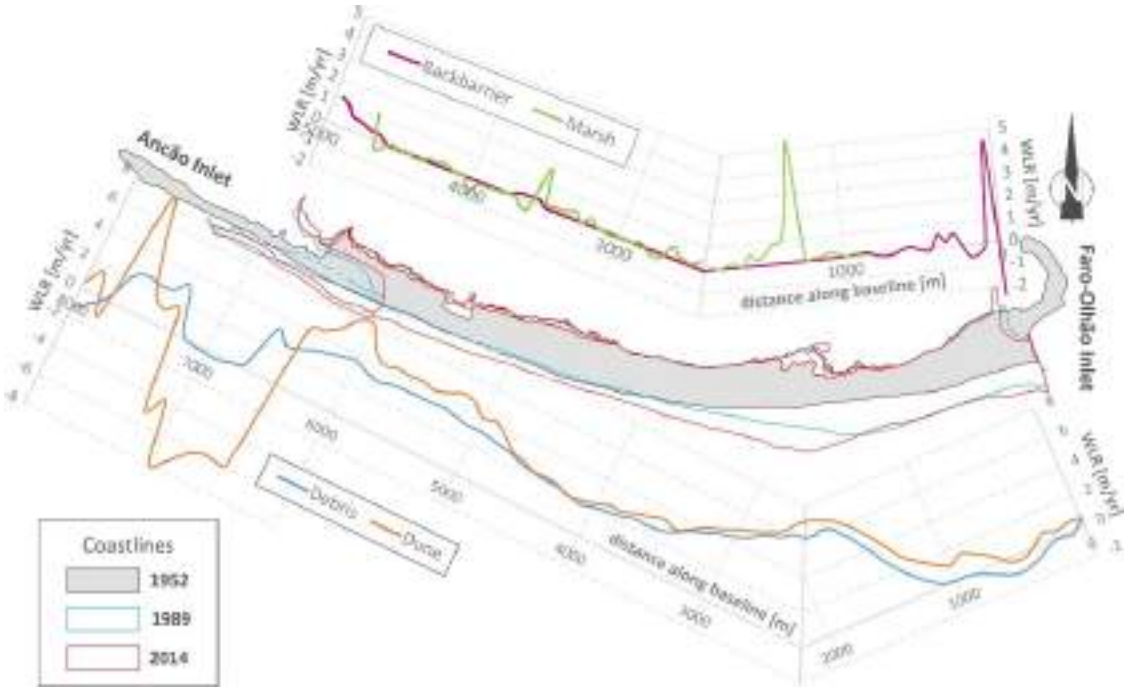

Figure 4 | Shoreline evolution rates (in m/yr) Barreta Island. The graphs in the top panel represent the rates for the backbarrier (purple line) and marsh (green line) and in the lower one the rates for the debris (blue line) and dune (orange line) (Kombiadou *et al.*, 2019).

The western area, affected by the migration of the Ancão Inlet, shows a seaward progradation and higher variability. In contrast, the back-barrier coast is very stable, and the mature marsh present in that area experienced either stability or growth. However, there was some local erosion in the east and west back-barrier edges as a consequence of both frequent channel dredging and the migration of the Ancão Inlet (Figure 4).

The barrier width is low and variable near the Ancão Inlet, where barrier and/or dune destruction were identified. In the west-central sector of Barreta Island, there was a dominance of accretion at rates of 2.4 m/yr and 3.2 m/yr for the barrier and dune widths, respectively. The widest barrier value (518 m) was found in the eastern region, in 1972 (Kombiadou *et al*., 2019) (see left panel at Figure 5).

Regarding the barrier areal evolution before the human interventions (relocation of Ancão Inlet and stabilization of Faro-Olhão Inlet with jetties), Barreta island experienced a growth process at an approximate rate of 10^4 m^2/yr (1873-1915: $9.8 \cdot 10^3$ m^2/yr; 1915-1952: $1.15 \cdot 10^4$ m^2/yr; 1873-1952:

1.06·10^4 m^2/yr). After the stabilisation of the Faro-Olhão Inlet, the island experienced growth at faster rates than in the pre-intervention period, and it only decelerated in the 1990s due to the likely impact of storms (see right panel at Figure 5).

The area located immediately updrift from the jetty (0-2.2 km) experienced fast growth up to 1985 (1.2·10^4 m^2/yr) followed by a slower progradation phase (3.5·10^3 m^2/yr) related to the westward shift of Santa Maria Cape. The area in the western flank of Barreta Island decreased after 2005 (-1.3·10^4 m^2/yr in the 2005-2014 period), reaching the 1972 values in 2014. These last results are a consequence of sediment starvation in Ancão and reduced sediment accumulation in Barreta, which causes low barrier growth in the west flank, showing similar rates as those existing before the construction of the jetties in the Faro-Olhão Inlet (Kombiadou *et al*., 2019).

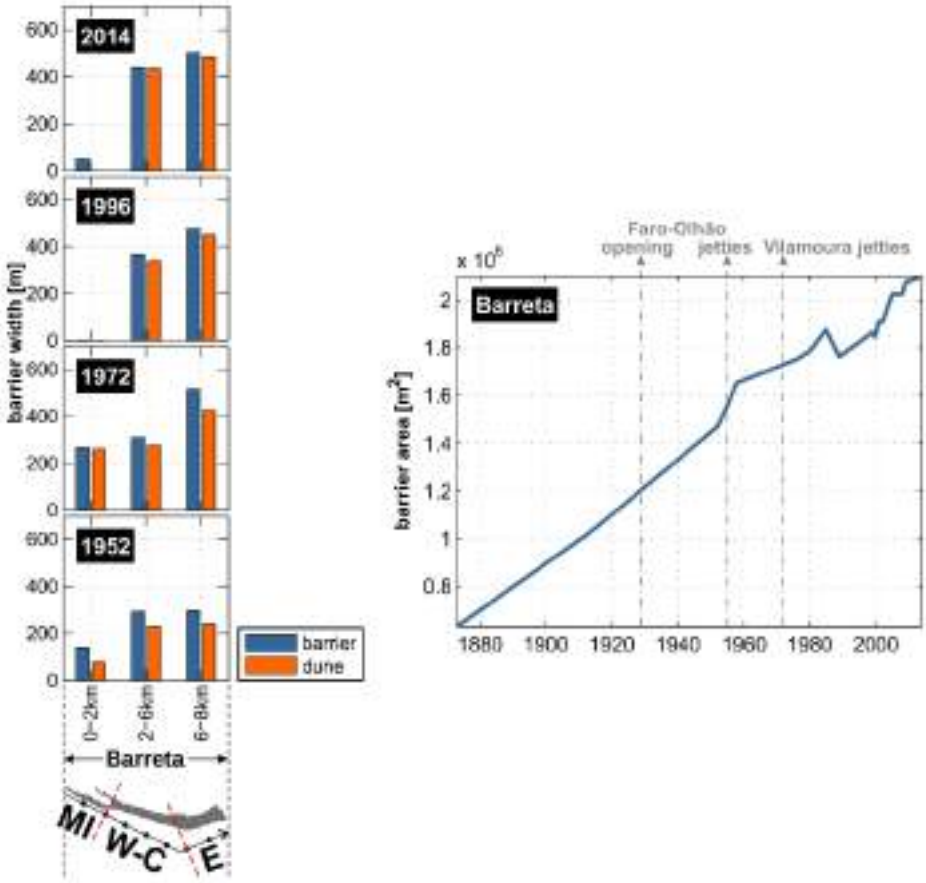

Figure 5 | Left: spatio-temporal evolution of barrier and dune widths (blue and orange bars, respectively). The map at the bottom (dtos spacing: 1 Km) show the selected barrier parts: Western (W), Central (C), and Eastern (E). Right: barrier area evolution (blue line). Major interventions are noted with grey dash-doe arrows (Kombiadou *et al.*, 2019).

Summarising, the evolution of Barreta Island showed a cross-shore growth trend as well as back-barrier and marsh stability. Barrier growth is the result of natural factors like longshore sediment transport, as well as artificial factors such as the jetty construction in the Faro-Olhão Inlet and the Ancão Inlet relocation. Based on the previous findings it can be stated that the evolution of Barreta Island from 1952 and 2014 has followed a regime of artificially enhanced growth, identified mostly in the updrift zone of the Faro-Olhão Inlet (Kombiadou *et al*., 2019).

4.2.2 Dune ridge construction processes

The central region of the island is the area where the most constant progradation and ridge formation rates were found during the entire period of study, in comparison with adjacent areas (see the Cape Zone area in Figure 6). In this region of Barreta, a total number of twelve ridges were developed during the analysed period (from 1929 to 2008), and they were grouped in five units for dating purposes. The morphological characteristics of the ridge units and the average metocean conditions for the corresponding time interval are shown in Table 2 (Herrero *et al*., 2020). According to previous findings, the lower ridges present in Barreta Island (Units 3 and 5) coincide with faster progradation rates. Contrarily, the higher foredunes (Units 1 and 2) appear to be associated to slow progradation rates.

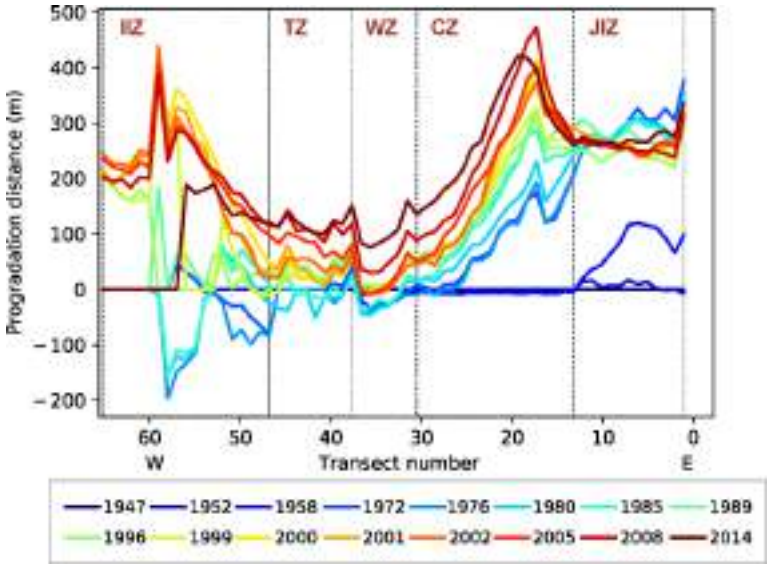

Figure 6 | Coastline progradation along Barreta island, from west (left-hand side) to east (right-hand side). The island is divided into five sectors marked on the plot (IIZ = Inlet-influenced zone, TZ = Transition Zone, WZ = West Zone, CZ = Cape Zone, and JIZ = Jetty-influenced Zone), while the colour coding of the flights is given in the legend (Herrero *et al*., 2020).

Table 2 | Morphological characteristics of the ridge units and average meteocean conditions for the corresponding time interval (Herrero *et al.*, 2020)

UNIT	UNIT 1	UNIT 2	UNIT 3	UNIT 4	UNIT 5
Nº of ridges	4*	3	2	2	1
Mean height (m)	5.63 ± 1.25	4.83 ± 0.59	4.44 ± 0.56	4.19 ± 0.28	3.78 ± 0.29
Mean width (m)	70	100	75	70	40
Time interval	1929**-1958	1959-1976	1977-1989	1990-2005	2006-2008
Ridge generation time (years per ridge)	14.5	6	6.5	8	3
Progradation rate (m/yr)	2.41	5.53	5.77	4.37	13.24
Aggradation rate (m^3/m^2 yr)	0.07	0.07	0.09	0.06	0.19
Winter crosshore wave power (m^2s/yr)	-	9770	9971	11154	10074
Winter longshore wave power (m^2s/yr)	-	9065	9233	8327	5680
No of aeolian sediment transport events/yr	-	61	54	55	38

Potential aeolian sediment transport ($m^3/m/yr$)	0.012	0.012	0.018	0.003

* only 2 of the ridges extend along the entire unit while the other 2 ridges cover only a part of it as they represent a lateral extension of ridges within the adjacent eastern zone.
** assuming the unit started growing after the opening of the Faro-Olhão Inlet.

The wind intensity did not show significant fluctuations during the period of study. However, strong events occurred during the formation of Unit 2, 3, and 4; and furthermore, the highest potential aeolian sediment transport (recorded during the formation of Unit 4) does not coincide with higher ridges, so additional factors such as sediment supply or storms may also influence the ridge formation processes (Herrero *et al*., 2020).

The identified ridges and corresponding unit areas in the central region of the Barreta Island are shown in Figure 7. The maximum run-up level was 4.1 m above MSL (estimated as the one exceeding the 0.99 quantile of the run-up levels from 1958 to 2008, plus the storm surge level associated with a 10-year return period). This value was the threshold chosen to distinguish the upper limit of the wave-driven constructive processes within the beach profile from the aeolian ones (see dotted line in the bottom panel of Figure 7). The results show that ridge units with mean elevations above this value (Units 1, 2, and 3) have significant aeolian contribution during their construction, and thus they are considered to be foredune ridges. Conversely, those ridges with mean elevations below or close to 4.1 m are expected to have been constructed under the action of marine processes, and are defined as beach ridges (Units 4 and 5); however, it is likely that their construction was also influenced by aeolian processes as accretion occurred and they have been established far away from the sea.

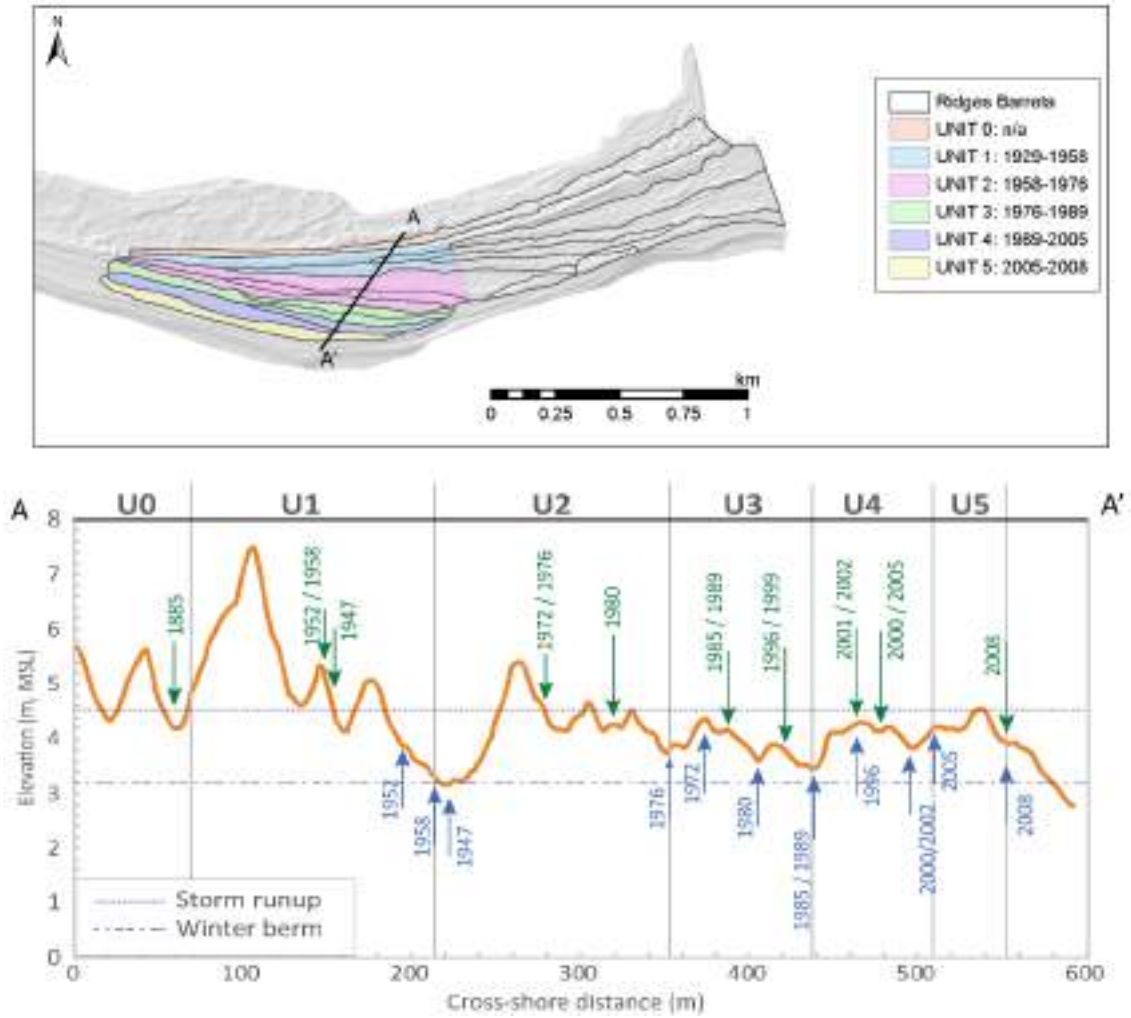

Figure 7 | Identification of the 17 ridges with support of LiDAR data (upper panel). The corresponding units withing the Cape Zone Santa Maria are pointed as colour polygons. The bottom panel shows an example of a cross-shore profile, intersecting the ridges within this area. The evolution of the position of the coastline, inferred from the position of vegetation line (in green) and from the high water mark (in blue), is highlighted (Herrero *et al.*, 2020).

5 | Dune cover evolution

5.1 Methods

5.1.1 Data collection

The degradation of the vegetation cover present in the grey dunes at Barreta Island was investigated using different remote-sensed data from 2008 to 2020: orthophotos, Google Earth images, and high-resolution mosaics derived from UAS surveys, all of them georeferenced to the PT-TM06/ETRS89 coordinate system. These datasets were used to visually identify the beginning and location of the degradation (the degraded areas identified are hereafter referred as DA), to classify the vegetation cover in the area, and to quantify the areal extent and the spatiotemporal changes of the different vegetation types across the area during the period of study. Some of the datasets (2014 4-band orthophoto) allowed the computation of NDVI (Normalized Difference Vegetation Index) map that was also used for classification purposes and to further assess the changes in vegetation health. Table 3 depicts the datasets used as well as their characteristics.

Table 3 | Datasets used for the dune cover analyses and their characteristics (O = Orthophoto, GE = Google Earth, P4P = Phantom 4 Multispectral).

Year	Month	Method	Resolution (m x m)	Island Cover	Dune cover analyses		
					DA Identification	Areal vegetation changes	NDVI maps
2008	Oct	O	0.1 x 0.1	Full	o	o	
2009	Nov	O	0.07x0.07	Full	o	o	
2013	Apr	GE	0.25x0.25	Full	o		
2014	Ago	O	0.1x0.1	Full	o	o	o
2017	Nov	GE	0.25x0.25	Full	o		
2019	Nov	Mavic 2 Pro	0.02x0.02	Partial		o	
2020	May	Mavic 2 Pro	0.02x0.02	Partial		o	
		P4M	0.05x0.05	Partial			o

The orthophotos were already available and obtained from different Portuguese institutions already mentioned in Section 4.1. The Google Earth images (2013 and 2017) were downloaded and georefenced using control points in ArcMap for complementing the available orthophotos. The orthophotos and Google Earth images allowed to analyse the covering of the whole island while the UAS surveys offered information of the western and eastern DAs (see the red and blue polygons in Figure 8, respectively).

The equipment used and the characteristics of the UAS surveys are shown in Table 4 and Figure 9. The permits to fly UAS in this region, the Ria Formosa natural park, were granted by different Portuguese Institutions: ANAC (Autoridade Nacional da Aviação Civil), ANN (Autoridade Aeronáutica Nacional), ICNF (Instituto da Conservação da Natureza e das Florestas), and the Capitania Marítima do Porto de Faro. The RGB and multispectral images acquired were processed with Structure-from-Motion (SfM) algorithms using Metashape, and the projects were georeferenced using the coordinates of evenly spaced GCPs that were measured using a RTK-DGPS (see the configuration of the GCPs in Figure 9).

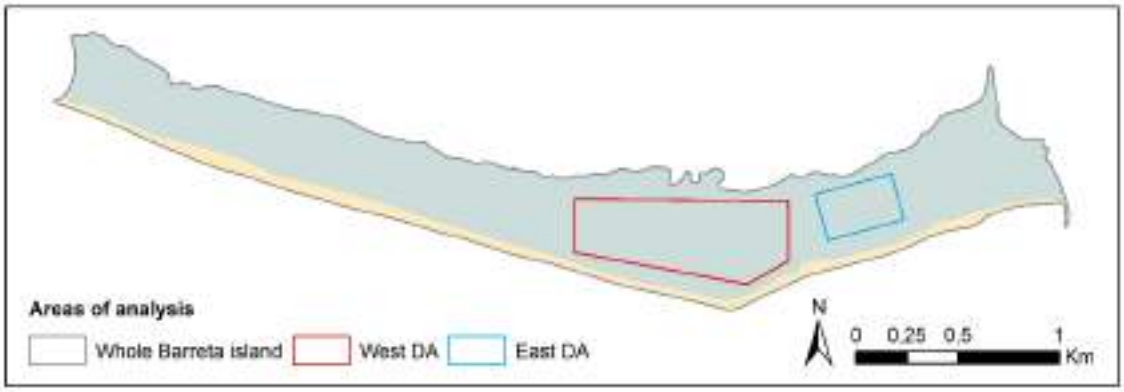

Figure 8 | Areas of analysis: whole Barreta island (WB), West and East DAs.

Table 4 | Characteristics of the UAS surveys performed.

Date	Equipment			Flight and camera parameters		
	Platform	Sensor		Flight Height (m)	Front-side overlap (%)	GCPs
		Type	Resolution			
Nov 2019	Mavic 2 Pro	RGB	20 Mpx	90	75 - 75	66
May 2020	Mavic 2 Pro	RGB	20 Mpx	90	75-70	64
	P4 Multispectral	RGB + Multispectral	2.12 Mpx	90	75-70	

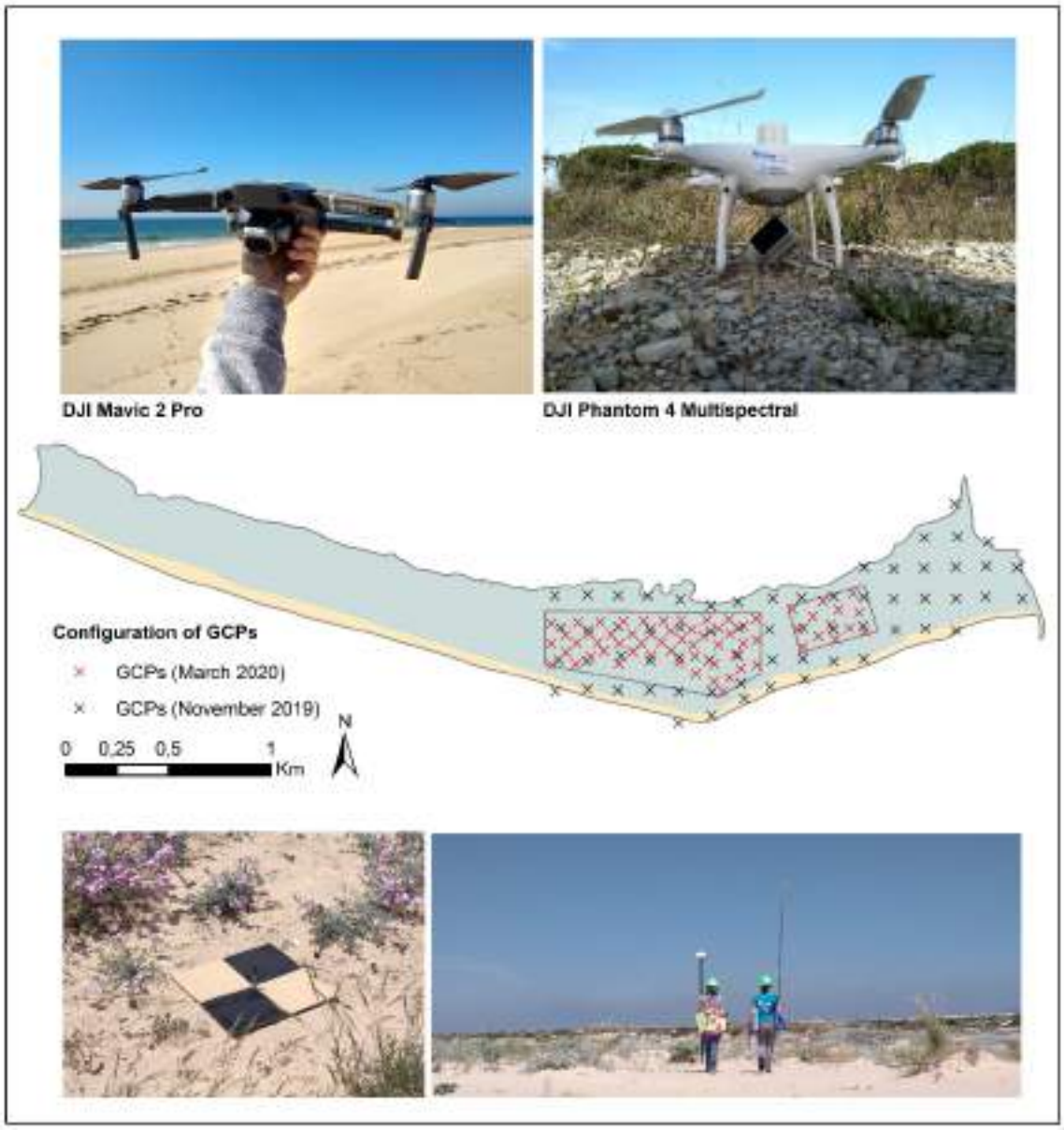

Figure 9 | Drone platforms used for the surveys, distribution of GCPs in November 2019 and May 2020, example of GCP used and RTK-DGPS surveys (from top to bottom).

5.1.2 Classification of images

To identify vegetation types and changes in cover in the area (2008, 2009, 2013, 2014, 2017, 2019 and 2020 datasets) the vegetation was classified using different methods. The first image classification method was performed using the unsupervised classification Tool (3 classes) within the Spatial Analyst Tools in ArcMap. The three vegetation classes distinguished in the datasets are the following (the plant species included in each class are depicted in Table 5):

- Class 1: Relatively healthy shrub vegetation
- Class 2: Healthy/degraded herbaceous vegetation (and degraded shrub from Class 1)
- Class 3: Bare soil (sand)

Table 5 | Plant species included in Class 1 and Class 2.

Class 1	
	
Artemisia campestris subsp. maritima	*Seseli tortuosum* L.
	
Helichrysum italicum subsp. picardi	*Thymus carnosus*
Class 2	
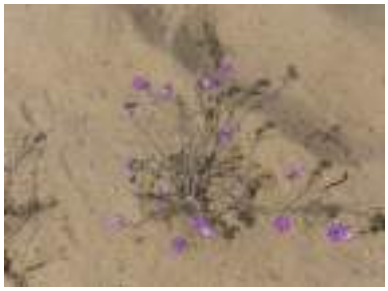	
Malcomia littorea	*Paronychia argentea*
	
Lotus creticus	*Corynephorus canescens*

Vulpia alopecuros

Medicago marina L.

Crucianella maritima L.

Silene nicaeensis

Pancratium maritimum

Ononis variegata L.

Othanthus maritimus

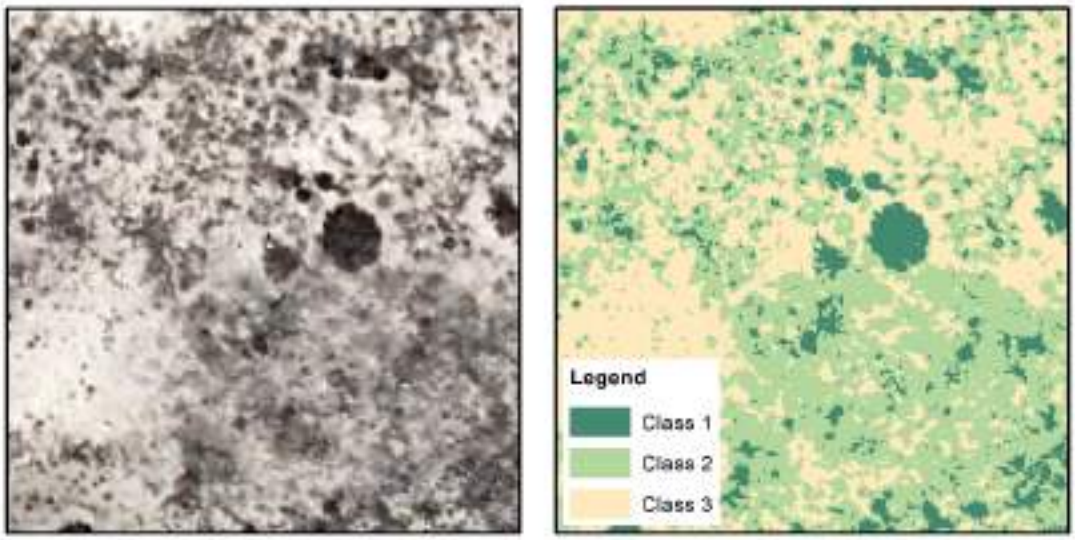

Figure 10 | Example of the 3 classes that result after computing the unsupervised classification. Class 1 is shrub vegetation, class 2 corresponds to herbaceous plants, and class 3 to bare soil or sand.

It must be noted that the already damaged shrub vegetation was classified as herbaceous vegetation, so Class 2 includes both healthy/degraded herbaceous vegetation and degraded shrub, which requires carefull attention during the analysis of results.

The second classification method used an NDVI map that was built using the 4-band 2014 orthophoto and the Raster Calculator Tool in Arcmap. It was computed according to the following expression:

$$\mathrm{NDVI} = \frac{\mathrm{NIR} - \mathrm{R}}{\mathrm{NIR} + \mathrm{R}}$$

where NIR and R correspond to the Near Infrarred and the Red bands, respectively. The NDVI is a common indicator to identify vegetation and to give information regarding its health. Healthy vegetation generally displays NDVI values close to 1 (higher NIR reflectance than R), while not so healthy vegetation displays NDVI values still above 0 although of smaller magnitude (higher R reflectance). This NDVI map was then reclassified into the abovementioned three classes according to the reflectance thresholds of each type, which where previously identified in the NDVI map (see Figure 11). These are the following:

- 1 < NDVI < 0.1 corresponding to Class 1
- 0.1 < NDVI < 0.015 corresponding to Class 2
- 0.015 < NDVI < -1 corresponding to Class 3

The multispectral imagery obtained during the UAS survey in May 2020 could not be used for image classification purposes, as different vegetation types exhibited same NDVI values, making it difficult to rely on it. However, the 2020 NDVI map was used to assess changes in vegetation health (see section 5.1.5) and it will be used also as a baseline mostly to assess possible vegetation recovery after the application of future conservation measures.

The accuracy of both classification approaches was performed using a set of 80 random points along the island (see Figure 12) and following the same procedure as in Jackson *et al.* (2019). The previous sample size was estimated based on binomial probability theory for an expected accuracy of 95% and an allowable error of 5%.

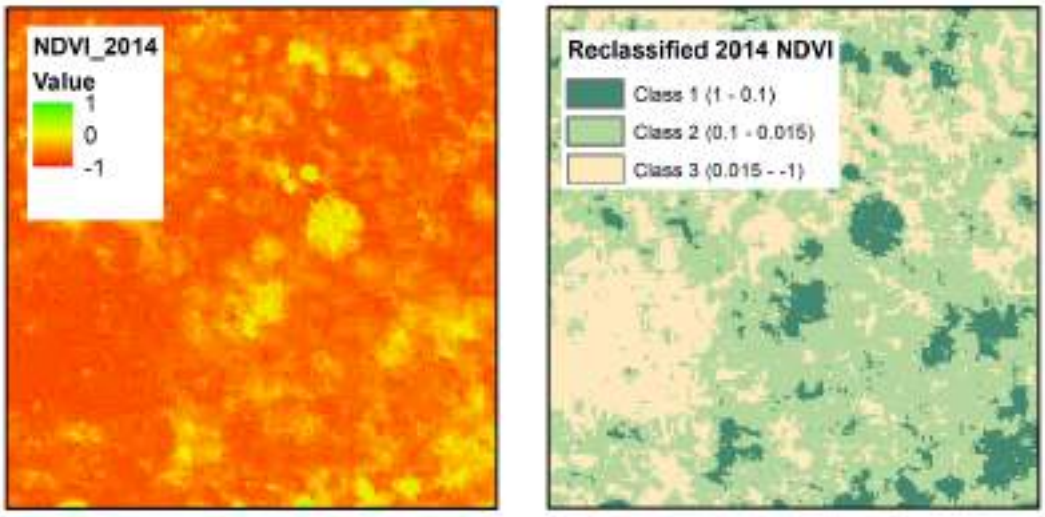

Figure 11 | Example of the reclassified 2014 NDVI map according to the different vegetation thresholds.

An error matrix was build comparing the classified values in each point of every dataset to the classification criteria of an observer in the same points (reference data), thus determining the degree of discrepancy among classes. This error matrix approach allowed the calculation of several statistics to assess the classification accuracy: the agreement accuracy, omission and commission errors, overall accuracy, and Kappa coefficient (Sen, 1968; Cohen, 1960). These are explained below:

- The agreement accuracy represents the probability (%) of a reference pixel being correctly classified.
- Omission error: represent pixels that belong to the reference class but fail to be classified into the proper class.
- Commission error: represents pixels that belong to another class but are labelled as belonging to the class.
- The overall accuracy represents the total classification accuracy.
- The Kappa coefficient is a discrete multivariate technique to assess the classification accuracy. It ranges from 0 to 1. Kappa coefficient values below or equal 0.40 indicate poor agreement, kappa values falling between 0.40 and 0.75 indicate an intermediate to good extent of agreement, while Kappa values above 0.75 indicate excellent agreement (Fleiss *et al*., 2013).

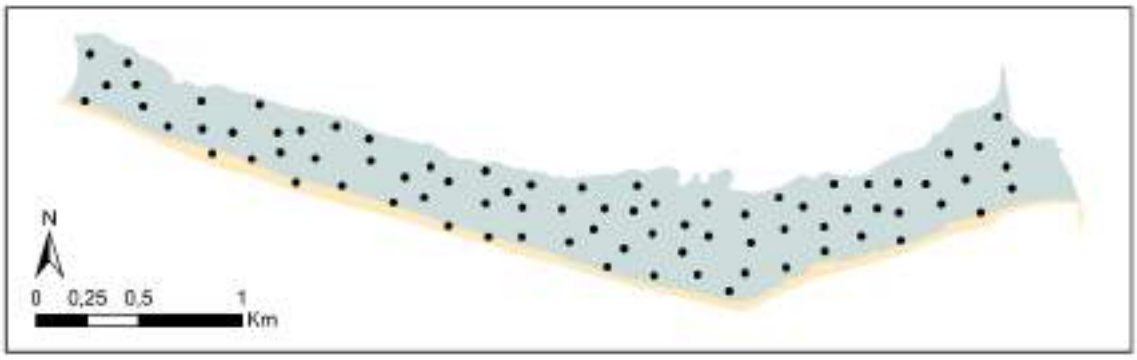

Figure 12 | Reference data used for the accuracy assessment of the image classification.

5.1.3 Dune cover analysis

To quantify the spatiotemporal evolution of the vegetation cover, the areal extent of each vegetation class was computed multiplying the total number of pixels counted for each class by the corresponding raster cell size using the Field Calculator Tool in ArcMap. This was done for every dataset, classification method, and area of analysis (whole Barreta Island, and West and East DAs).

5.1.4 Dune degradation index

To unify criteria for the computation of the health vegetation index, every classified dataset was transformed into a raster of 1x1 m cell size. The health vegetation index was then evaluated within square areas of 100 m^2 in every dataset. These areas were defined using a regular grid (10x10 m cell size) that was built using the Fishnet Tool in Arcmap. Class 3 (bare soil) was selected to indicate the degree of health/disturbance in the area as it was the class that best represented the observed degradation in the island. The area and percentage cover of Class 3 in each dataset was calculated multiplying the number of pixels counted for that class by the area of the grid cells (100 m^2). The optimal Class 3 percentage cover that was selected for the degradation index was 35%, for grey dunes. This value represents the optimal grey dune composition (with regards to Class 3) back in 2008, before the start of the degradation. It was obtained by observing the frequency of Class 3 values in the area, recognized as having a healthy grey dune composition, and by computing the mean of the Class 3 percentage cover values.

Areas in the index maps showing percentage cover values of Class 3 above 35 % indicate some sort of disturbance, whereas areas with percentage values below it indicate a good grey dune composition. To interpret correctly the results, it must be noted that disturbance could be also be shown in areas naturally characterised by high cover of sand (*e.g.* mostly beach or immature dunes) since the density of vegetation cover at those areas is not as high as in grey dunes. To illustrate better the gradients in the degree of grey dune disturbance, the vegetation index was represented according to three ranges:

- 0 – 35 % cover indicating an optimal grey dune composition
- 35 – 55 % cover indicating partially disturbed grey dune composition
- 55 – 100 % cover indicating disturbed grey dune composition, beach area and/or immature dune.

In order to identify the areas experiencing gain and/or loss of sand cover (Class 3), the index maps were complemented with analyses of Class 3 percent cover change (sand gain/loss), which were computed from consecutive datasets and using the Raster Calculator Tool within Arcmap.

5.1.5 Dune health evolution

In order to examine the dune vegetation health, the 2014 and 2020 NDVI maps were used to compute vegetation reflectance changes in time using the Raster Calculator Tool in GIS.

5.2 Results

5.2.1 Classification accuracy

The parameters used to assess the classification accuracy (both using the unsupervised classification and the NDVI) are depicted in Table 6. As it can be observed, the kappa parameter is always 0.90 or above, which is a magnitude considered to represent an excellent agreement

according to the scale proposed by Fleiss *et al*. (2013). The overall accuracy also showed an excellent classification, as it always presented values above 80%. It should be taken into consideration that the fact of getting good accuracy values does not mean that the values within datasets are comparable, as they refer to a comparison against points of the same dataset. Each dataset can have their intrinsic characteristics (light, reflexion, plant seasonality) turning dififcult the comparion between different datasets/years even if all of them have an excellent individual accuracy.

Regarding the unsupervised classification, it was generally observed that the lower agreement accuracy was found in Class 2, as the herbaceous vegetation is sometimes confused with bare soil (Class 3) and degraded shrub (Class 1). Regarding the omission error, it is lower in Class 3, as the bare soil (Class 3) is easily distinguished. Classes 1 and 2 showed the highest omission errors due to the influence of the image colour and light exposure, which make these classes to be classified as different ones. These factors also influenced the commission errors, which in general were higher in Class 3, as some of the herbaceous vegetation from Class 2 are often classified as bare soil.

Table 6 | Results from the classification accuracy assessment.

CLASSIFICATION ACCURACY												
Unsupervised classification												
Year	**Area**	**Agreement accuracy**			**Ommision Error**			**Commision Error**			**Kappa**	**Overall Accuracy**
		Classes			**Classes**			**Classes**				
		1	***2***	***3***	***1***	***2***	***3***	***1***	***2***	***3***		
2008	WB	68.4	93.0	94.4	31.5	6.97	5.5	7.1	14.8	10.5	0.90	87.5
2009	WB	91.3	60.7	100	8.69	39.2	0	0	10.5	27.5	1.0	83.75
2013	WB	92.8	88.2	96.8	7.1	8.8	3.1	7.1	6.2	8.8	0.91	92.5
2014	WB	77.7	70.9	100	22.2	29.0	0	0	21.4	29.0	1.0	81.25
2017	WB	100	86.9	100	0	13.0	0	0	0	26.0	1.0	92.5
2018	WB	70.5	82.6	100	29.4	17.3	0	7.6	11.6	70.8	0.90	83.75
2019	E	100	66.6	100	0	33.3	0	0	0	50	1	80
	W	100	81.1	100	0	18.1	0	0	0	60	1	86.6
2020	E	-	66.6	100	-	33.3	0	-	0	66.6	1	80
	W	100	88.8	100	0	11.1	0	0	0	83.3	1	93.3
NDVI classification												
Year	**Area**	**Agreement accu-racy**			**Ommision Error**			**Commision Error**			**Kappa**	**Overall Accuracy**
		Classes			**Classes**			**Classes**				
		1	***2***	***3***	***1***	***2***	***3***	***1***	***2***	***3***		
2014	WB	61.1	83.3	96.1	33.3	16.6	3.8	0	18.9	81.2	1	82.5

The previous factors (image colour and light exposure) also impacted the accuracy of the NDVI-based classification. Besides, it must be taken into account that different vegetation classes may share common NDVI reflectance values due to different degrees of degradation. This overlap made it complicated to establish reflectance thresholds to classify the images in different vegetation types, specially in the 2020 NDVI map.

5.2.2 Areal evolution of vegetation classes

In 2014 there was a clear increase in bare soil (Class 3) in two areas of the central part of Barreta with respect to the previous years (Figure 13 and 14). These areas correspond to the western and eastern DAs that were visually identified from the orthophotos. From 2014 to 2017 the maps showed a slight increment in the cover of Class 3, which continued increasing until 2020 as shown in Figure 14. Before 2014, there was a small area in the west part of the West

DA that could indicate the start of the degradation (see the 2009 and 2013 maps in Figure 14) but this could be also a result of different image colour and/or light exposure. In fact, some areas of the 2009 map are masked as they were influenced by a cloud shadow that was easily distinguished, so the classified vegetation in these areas may differ from reality.

Figure 13 | Dune classification maps for the whole Barreta Island derived from the unsupervised classification.

The detailed view of the DAs (western and eastern; Figure 14) made even more obvious the observation of changes on the vegetation, namely after 2013, at those areas, but also the existing variability on classes classification, which can result from different images colours/reflectance.

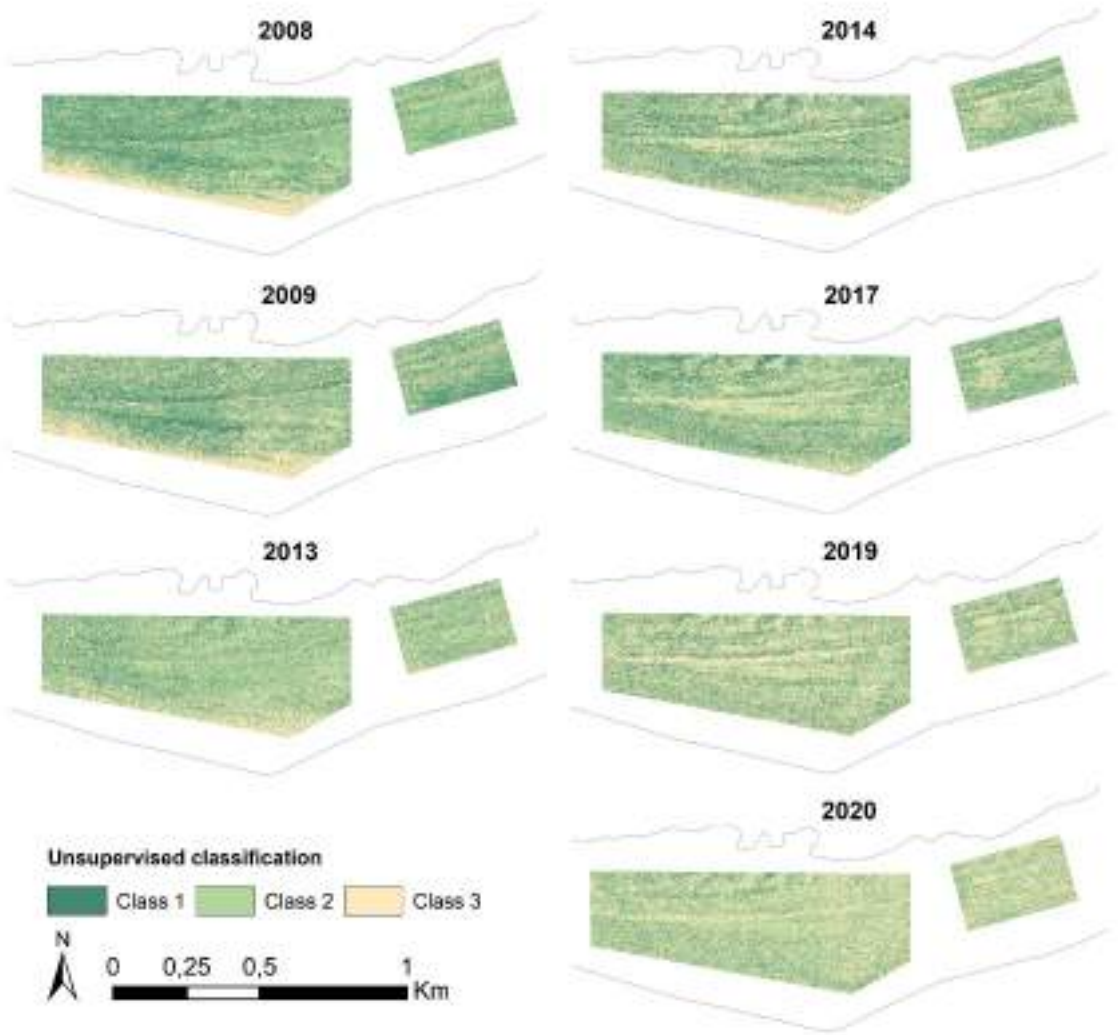

Figure 14 | Dune classification maps from the western and eastern DAs resulted from the unsupervised classification.

The areal cover of each class in each dataset was also computed. The cover of the different vegetation classes across the whole island fluctuated from 2008 to 2017, with no clear tendency of increase/decrease in any of the classes (see the upper panel in Figure 15 and Table 7). The most remarkable changes in cover were found in both the western and eastern DAs, which despite showing fluctuations, also exhibited a general trend of decrease in shrub vegetation (Class 1) and increase in bare soil or sand (Class 3) (Figures 15). The oscillations in time of each class are attributed again to the use of datasets of different nature and with different image colour and exposure.

Differences in cover of each vegetation class were found when comparing the unsupervised classification and the NDVI-based classification in 2014. For instance, the cover of Class 1 in the whole Barreta Island changed from 587933 to 339495 m^2 for the unsupervised and NDVI-based classifications, respectively (Table 7). These differences are quite high and mean that the methods cannot be directly compared one against the other.

Table 7 | Results from the unsupervised classification accuracy assessment in WB, eastern DA, western DA; and the NDVI-derived classification.

	Year	Cover (m^2)		
		Class 1	*Class 2*	*Class 3*
WB	2008	544484	845577	833368
	2009	646294	635862	941274
	2013	479126	808221	931021
	2014	587933	666742	968755
	2017	636667	794989	781424
	Year	**Cover (m^2)**		
		Class 1	*Class 2*	*Class 3*
EASTERN DA	2008	24259	56216	10391
	2009	36908	35589	18370
	2013	22540	47183	23152
	2014	26268	37675	26923
	2017	27425	42749	21735
	2019	20106	28122	32776
	2020*	10660	33460	30968
	Year	**Cover (m^2)**		
		Class 1	*Class 2*	*Class 3*
WESTERN DA	2008	123974	171685	62135
	2009	125309	117507	114977
	2013	88052	180072	97578
	2014	117763	132051	107980
	2017	106289	160586	95023
	2019	76046	113501	129624
	2020*	52352	155566	117195
	Year	**Cover (m^2)**		
		Class 1	*Class 2*	*Class 3*
NDVI	2014-WB	339495	790340	1093591
	2014-E	8497	33512	48854
	2014-W	89506	180346	87942

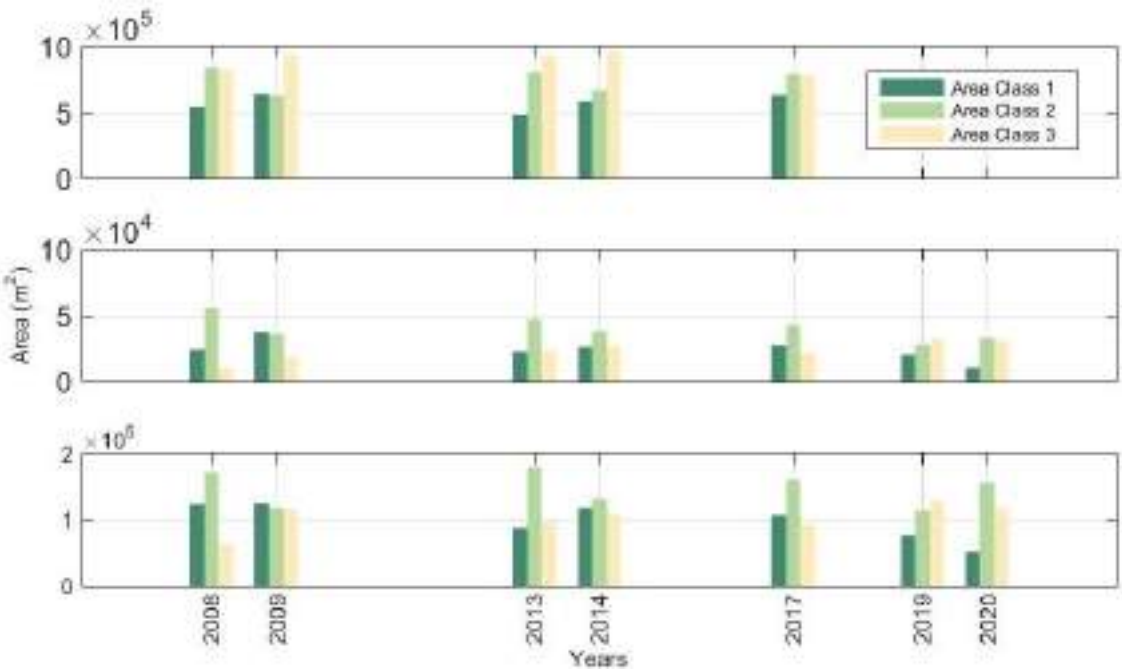

Figure 15 | Areal evolution of vegetation classes obtained from the unsupervised classfification at Barreta Island (upper panel), East DA (middle panel), and West DA (lower panel).

5.2.3 Vegetation index

At the beginning of the period of study, most of Barreta Island exhibited sand cover below 35%, which was considered as an optimal percentage cover of sand for the grey dunes according to the proposed index (see the green area in the 2008 map in Figure 16).

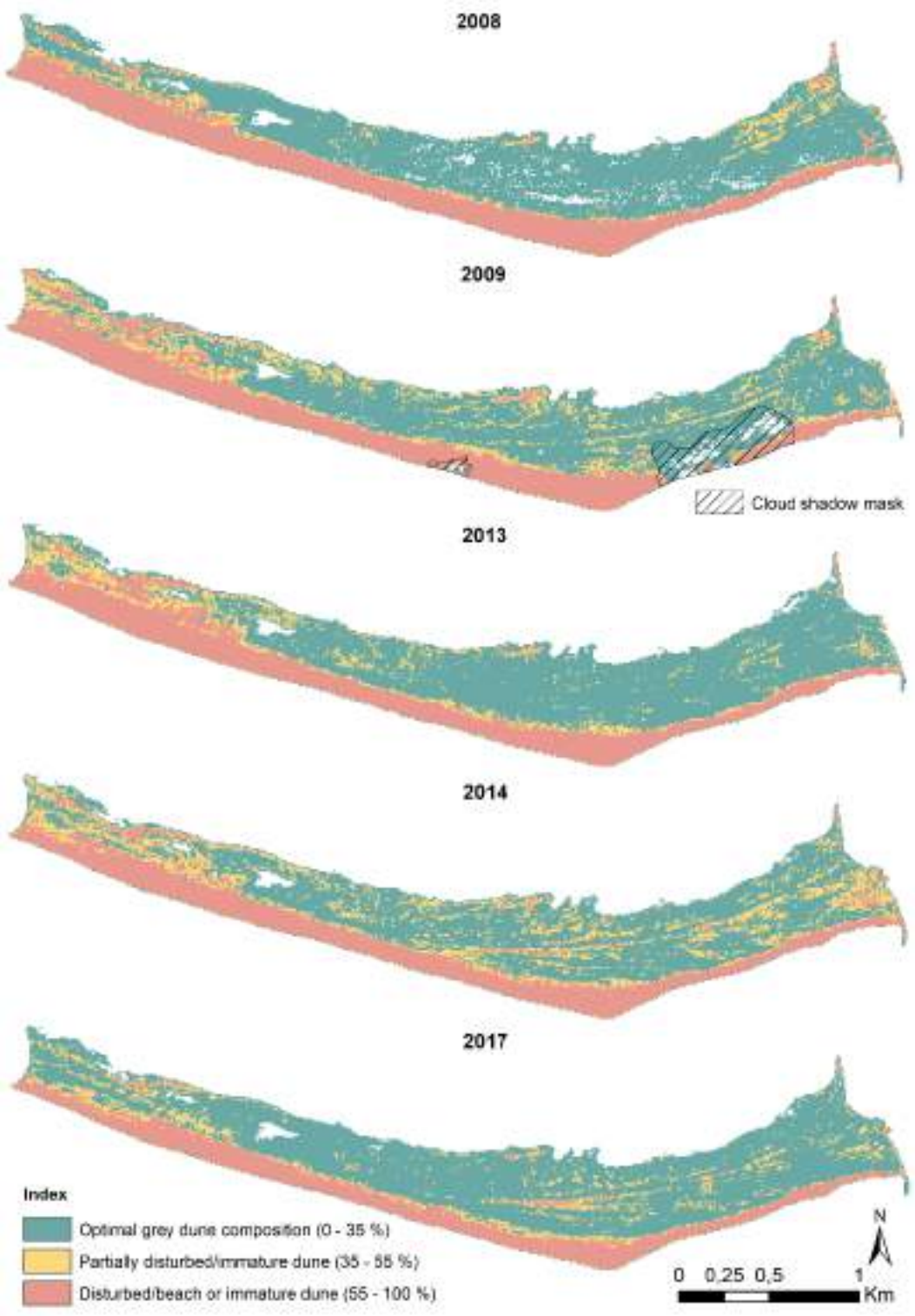

Figure 16 | Dune health maps for the whole Barreta island from 2008 to 2017. The white patches represent "no result".

Some exceptions to this are the entire beach area (sand cover above 55%) and the western end of the island, where the immature dune and the existing onshore aeolian transport increased the sand cover. In order to interpret correctly the index maps, these previous factors need to be taken into account.

No sign of significant grey dune disturbance is observed until 2014, with the exception of a small area in the easternmost part of the island nearby the restaurant location (see 2008, 2009, and 2013 maps in Figure 16) and some small areas showing partial disturbance (see yellow patches also in the 2008, 2009, and 2013 maps in Figure 16). However, in 2014 the dune ridges located at the central part of the island presented a clear disturbance (not attributable to aeolian transport of sand or human action) that persisted until 2017. The disturbance is more significant along the highest dune ridges of the two main DAs previously identified. From 2017 to 2019, the mentioned disturbance spread from the highest dune ridge to the north and south directions; however, the 2020 map showed a slight sand cover decrease (or dune recovery) probably related to the blooming of previously degraded herbaceous plants. This was likely linked to the precipitation that occurred in the early 2020 spring (see the western DA in the 2019 and 2020 maps in Figure 17). This fact also calls the attention to the need of understanding seasonal differences on vegetation when analysing this type of results, as yellow patches indicating partial disturbance may be attributed to natural seasonal vegetation shifts.

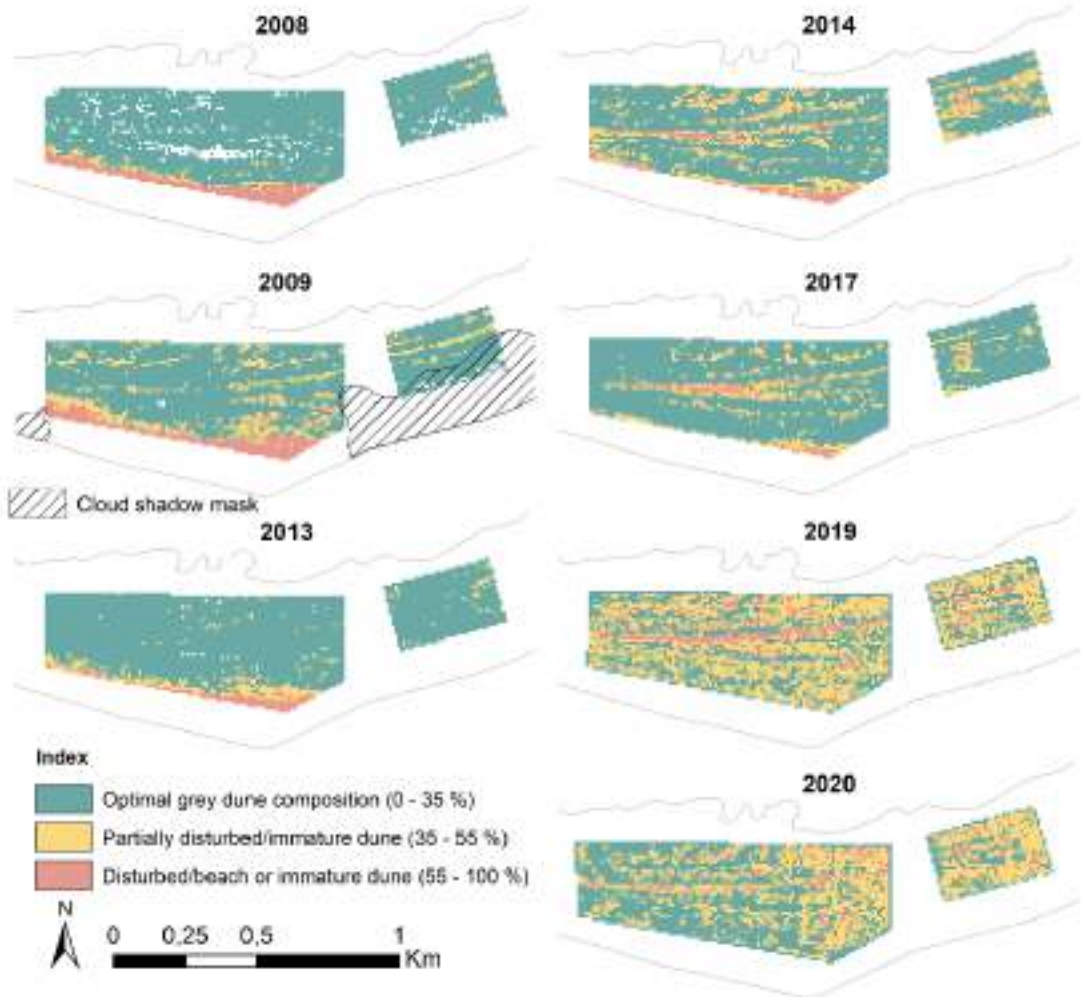

Figure 17 | Dune health maps for the West and East DA from 2008 to 2020. The white patches represent "no result".

The percentage of cover change of sand (Class 3) was also computed to complement the previous index maps and served to highlight the areas within the island that exhibited gain/loss of sand cover

during the period of study (represented in Figures 18 and 19 with blue/red colours, respectively). As indicated in the index maps, from 2013 onwards the central area of Barreta Island gained cover of sand due to the dune degradation, which was more accentuated again in the two main DAs along and near the highest dune ridge.

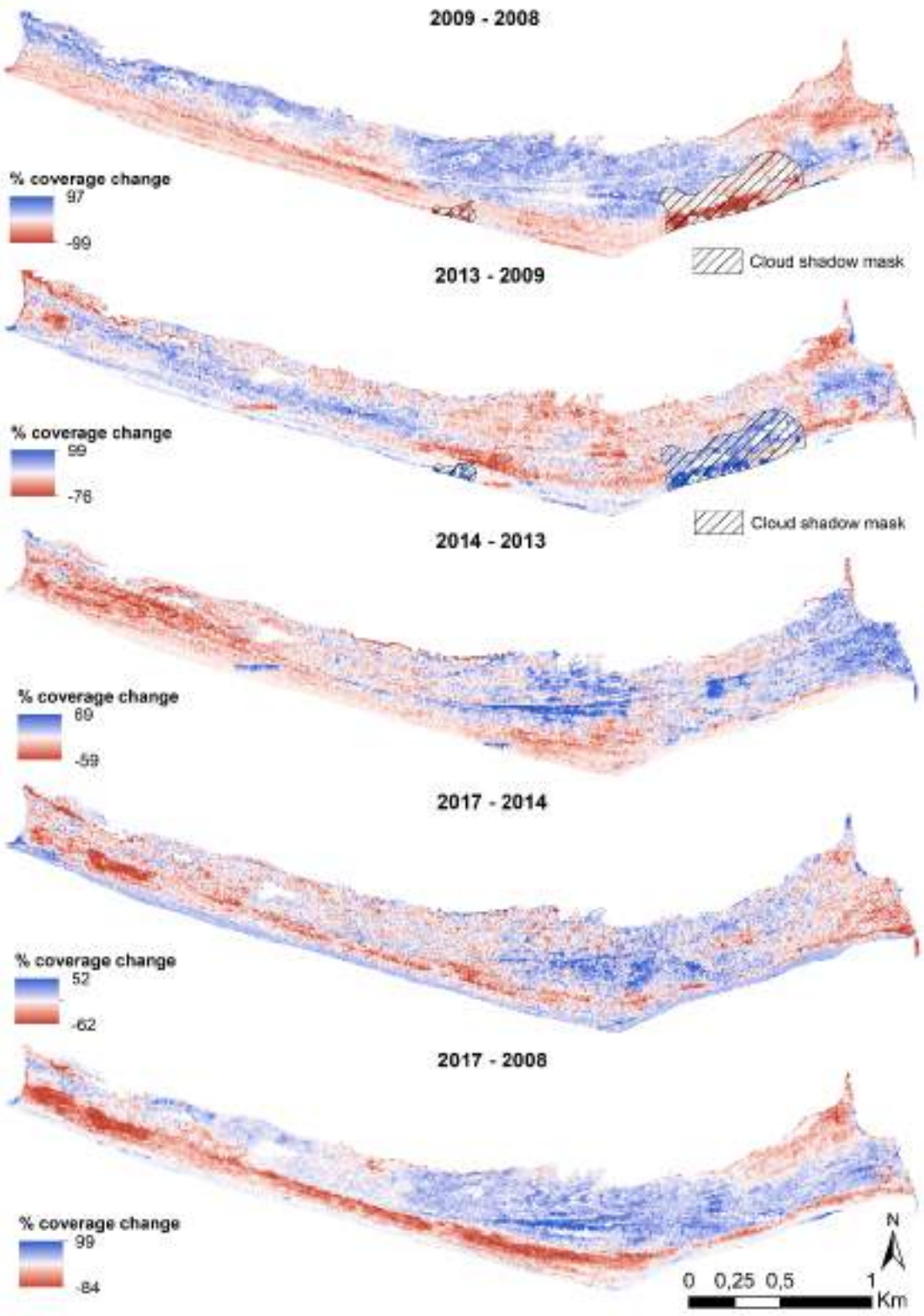

Figure 18 | Computed % change map for Class 3 (bare sand) in the whole Barreta island from 2008 to 2017. The areas experiencing gain and loss of % cover of Class 3 are represented by blue and red, respectively.

The remaining patterns showing gain/loss of sand cover in the island were mostly related to issues derived from the quality of the images, as well as from the actual seasonal variability in the vegetation and dune state. The 2020-2019 map in Figure 19 again showed a slight recovery in both western and eastern DAs, as the sand cover decreased due to the blooming of plants as a consequence of precipitation during spring.

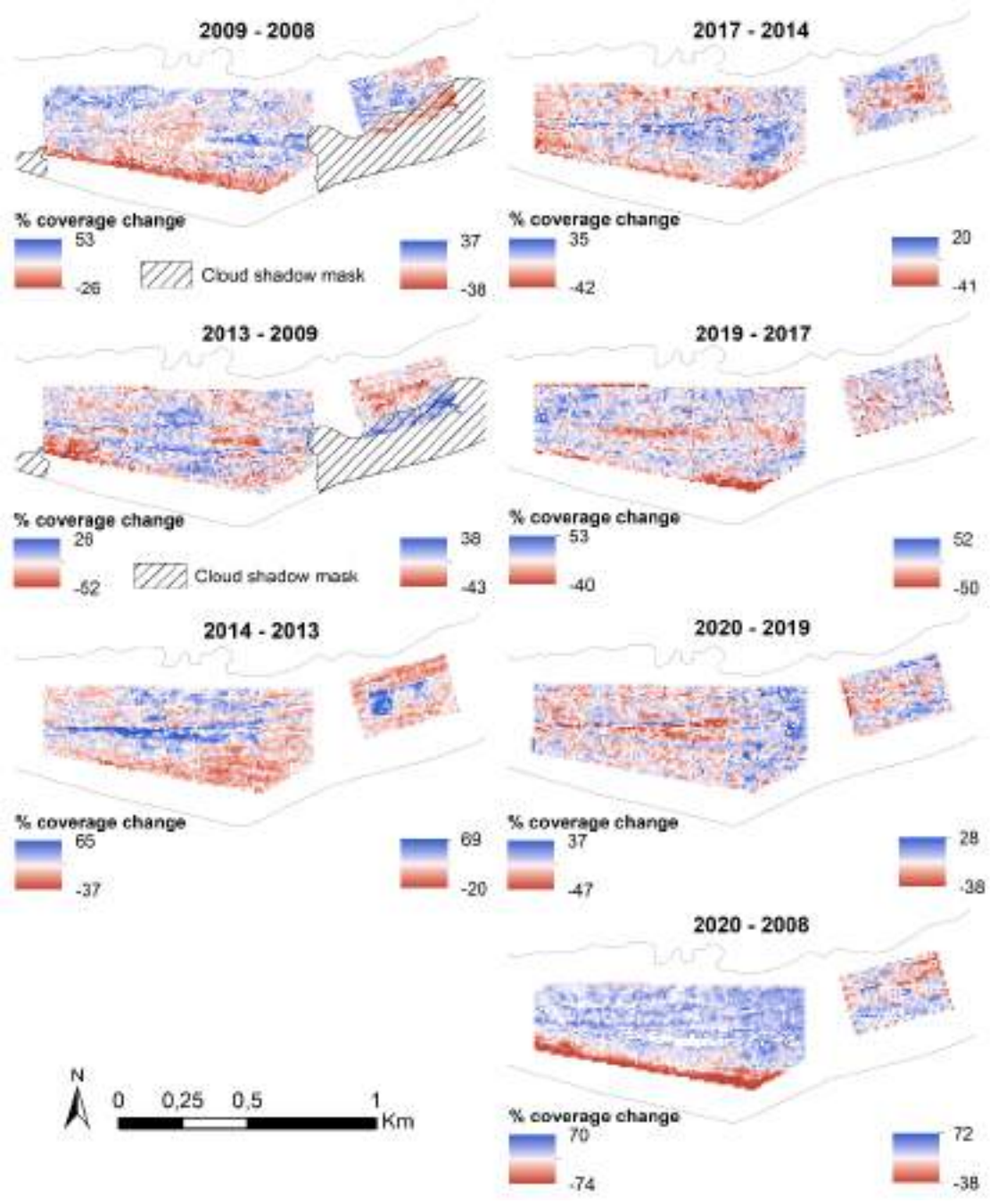

Figure 19 | Computed % change map for Class 3 (bare sand) in the West and East DAs from 2008 to 2020. The areas experiencing gain and loss of % cover of Class 3 are represented by blue and red, respectively.

5.2.4 Vegetation health based on NDVI

The computed 2014 NDVI map of the whole island showed an average NDVI value of 0.04. However, the NDVI values varied spatially along the island due to the existence of areas with

different vegetation types and cover (e.g. immature dune) as well as areas naturally influenced by aeolian transport (e.g. beach area) (upper panel in Figure 20). More examples of this variability were found in the region corresponding to the western DA, which showed an average NDVI value of 0.06 (superior to the average NDVI of the whole island). The central part of this region showed the lowest NDVI values (between 0 and 0.015, approximately), and this contrasted with both the adjacent areas to the North and South, where the vegetation exhibited a healthier state (NDVI values above 0.5). On the other hand, the region corresponding to the eastern DA in 2014 showed low NDVI values in general (average NDVI of 0.02), with the exception of a few locations.

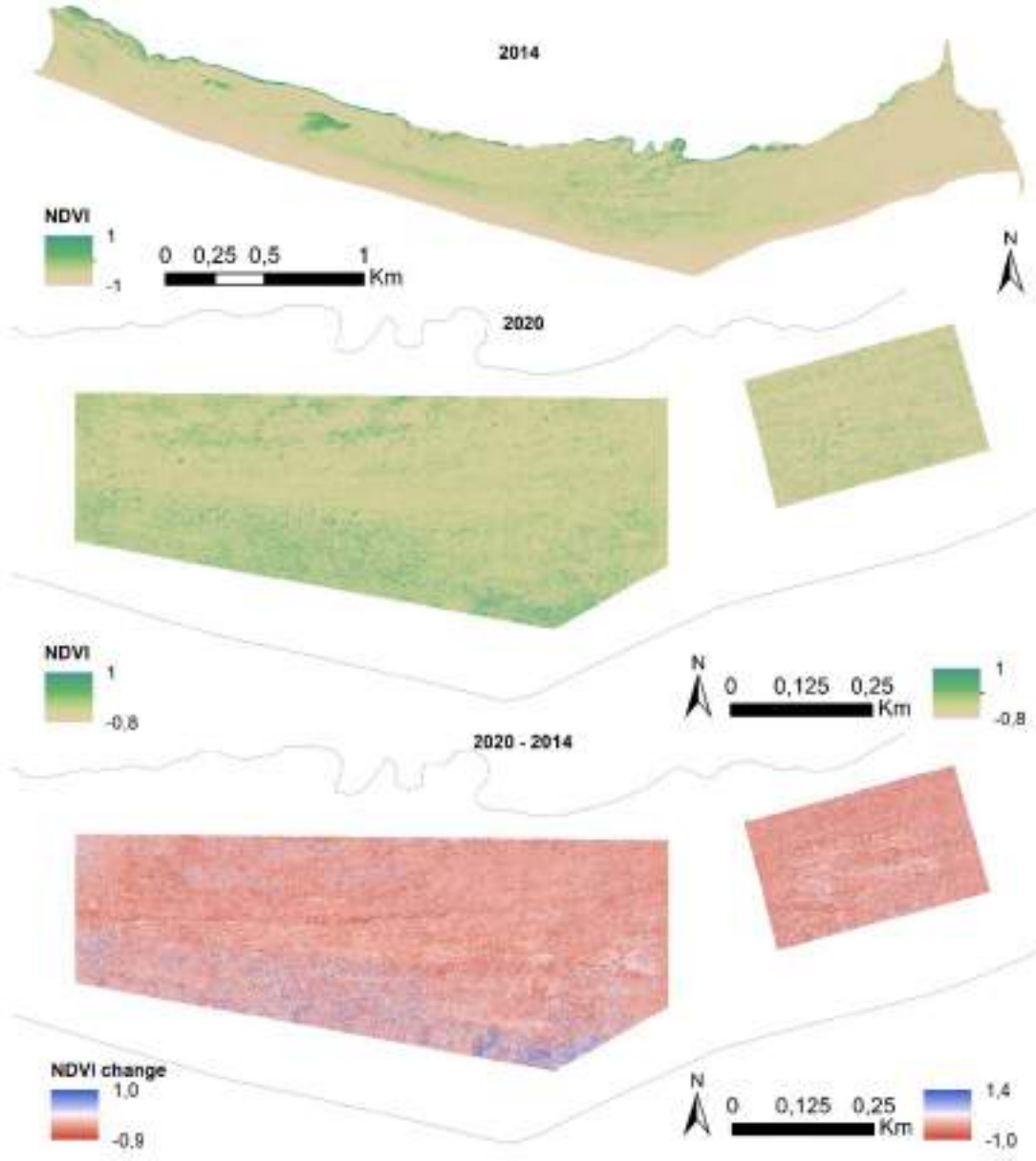

Figure 20 | 2014 and 2020 NDVI maps, and NDVI change map (2020 - 2014).

The previous NDVI spatial patterns seem to be maintained in 2020; however, the average NDVI values at both the western and eastern DAs in 2014 (0.06 and 0.02, respectively) contrasted with the average NDVI values found in the same areas in 2020 (middle panel in Figure 20), which are 0.14 and 0.10, respectively. This NDVI increase suggest a net recovery that may be explained by natural vegetation seasonal shifts that may occur from summer to spring, as the 2014 and 2020

datasets were obtained in August and May, respectively. The observed plant health recovery could be a consequence of the blooming of plants observed in May 2020, favoured by early spring rain events as stated before. The bottom panel at Figure 20 shows that the plant recovery (blue) was more significant in the areas to the North and South of the central part of the western DA, showing no clear pattern in the eastern DA. Despite the net recovery, degradation dominated spatially across both western and eastern areas (red) although at lower magnitudes than recovery, with the exception of some areas located along the highest dune ridge in the western DA (see the dark red patches at the bottom panel in Figure 20)

The analysis of plant health evolution needs to be carefully done as in some occasions the measured degradation and/or recovery of plants could be again a consequence of natural seasonal shifts in vegetation, and may not be attributable to external factors of disturbance (e.g. human or other type of interference in the habitat). To assess the real plant health evolution from year to year datasets obtained in the same month (or season) would be needed. Nevertheless, the datasets shown above provided useful information that will be complemented with upcoming seasonal UAS surveys. These will allow the distinction between natural seasonal vegetation degradation from disturbance attributed to other factors.

6 | Human pressure and occupation

Barreta Island is one of the best conserved and less frequented barrier islands in the Ria Formosa. Even so, it is subject to some human pressures that could cause additional disturbances in the different habitats, contributing to localised dune degradation.

6.1 Methods

In order to understand the contribution of possible human interference (activities and/or visitors) in the degradation of the different habitats, the infrastructures and human-derived signs present across the island were digitised as polylines and polygons in GIS using the available datasets (Table 3). These infrastructures namely include hard structures such as the jetties in the Faro-Olhão inlet, buildings such as fishermen houses and warehouses, a restaurant as well as wooden paths and trampling paths.

6.2 Results

The distribution of buildings and wooden paths did not change significantly during the period of analysis, with the exception of the fishermen houses located in the north-west of the island (Figure 21 a), which were removed in the late 2014 or early 2015.

Most of the trampling paths appeared in the surroundings of the fishermen houses and warehouses and near the restaurant (see the 2014 and 2017 maps in Figure 21 a and b).They were probably formed due to frequent and rutinary activities, although there are a few wooden paths connecting these areas to the beach. Similarly, there are also signs that indicate trampling from the main wooden path (see blue line in Figure 21) of the island to the lagoon beaches. No trampling signs were found connecting the main wooden path that crosses the island with the degraded dune ridges and the DAs.

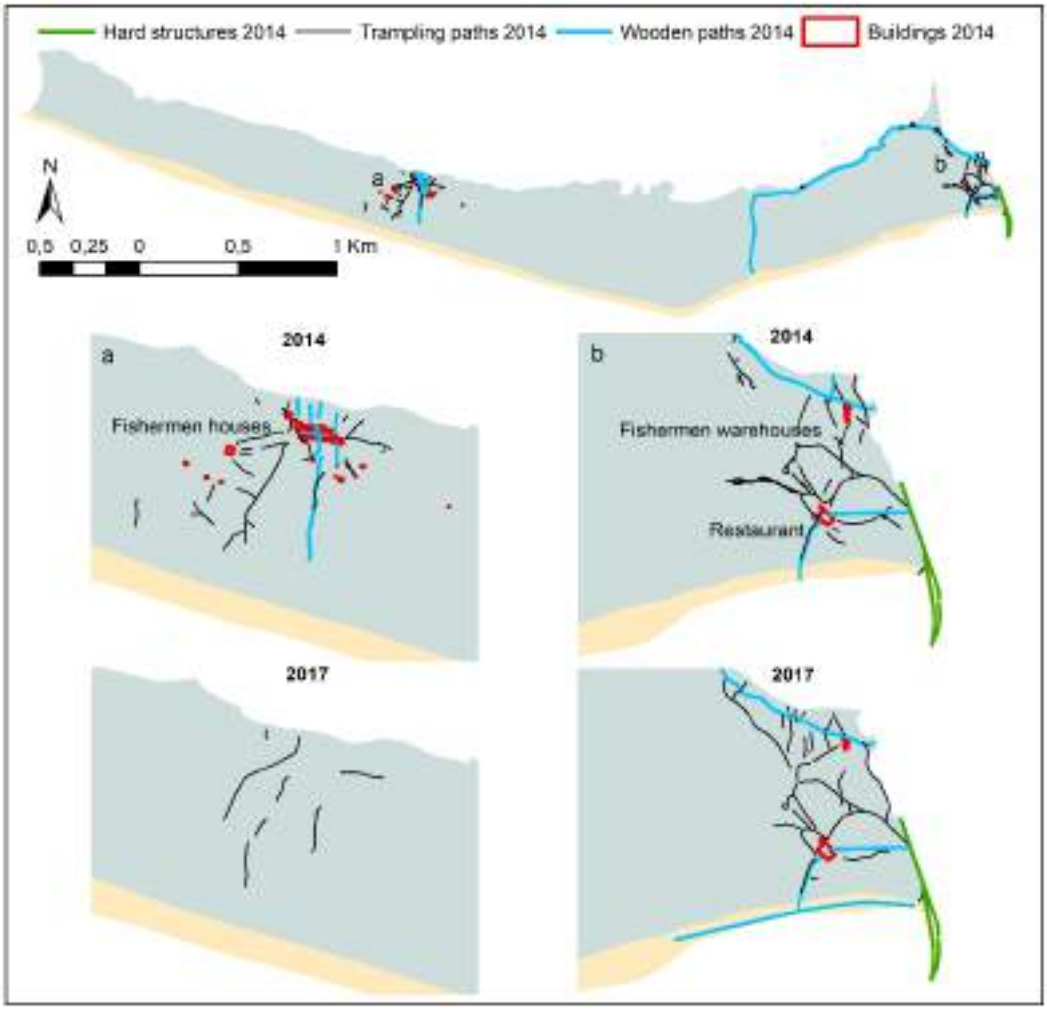

Figure 21 | Human occupation in Barreta island in 2014 and 2017.

7 | Gull pressure and occupation

7.1 Methods

In situ annual gull censuses performed by the University of Coimbra (2014-2019) and SPEA (2020) during the breeding season gave information regarding the population size of the different gull colonies and the spatiotemporal evolution of their main distribution areas in the island.

7.2 Results

The main distribution areas of of Yellow-legged gull and Audouin's Gull along Barreta Island were mostly located at central areas of the island (see the red and blue circles, respectively, at Figure 22).

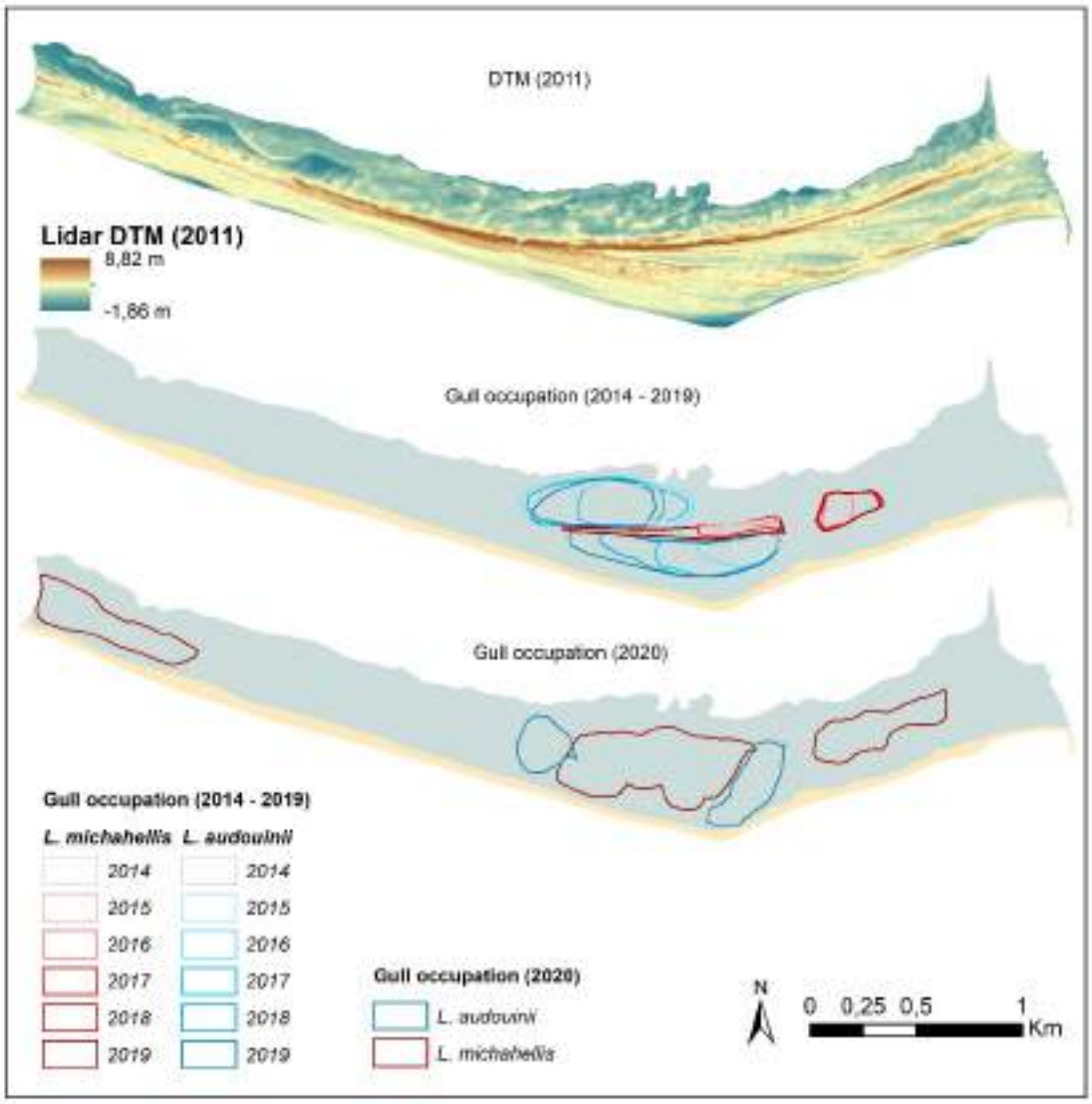

Figure 22 | Gull occupation in Barreta island from 2014 to 2020.

Yellow-legged gull *mostly* occupied the dune crests and surrounding areas at the DAs under study (between 2014 and 2019) and an additional low altitude area on the western part of the island from 2015 or 2016, approximately. Audouin's Gull was found mostly close to the *L. michahellis* population located in the central part of Barreta Island, but occupying the lower areas to the north and south of the highest dune ridge crest (2014-2020) or lateral areas (2020; Figure 22). It must be enhanced that the surveys from 2014-2019 and 2020 used different methodologies and thus the results also show some variability associated to the methods. From the 2014-2019 surveys it is observable that apart from some movements of the populations of gulls, the most relevant trend was the increase in the occupied area, by both species.

Regarding the population size of both colonies, Audouin's Gull was clearly superior to Yellow-legged gull during the whole period of study (Figure 23) and the difference is further increasing. Moreover, its population density was higher than Yellow-legged gull due to the fact that they occupy areas of smaller extent within the island. Both populations have gradually increased from 2014 to 2020, reaching their peaks and some stability between 2018 and 2020.

On the other hand, it is important to take into account that both species breed in sympatry during the breeding season (Matos *et al*., 2018) (mid April to mid July, approximately) in Barreta Island. During the non-breeding season Yellow-legged gull stays in the area while Audouin's Gull migrates southwards to West Africa (unpublished data from the University of Coimbra). This migratory path has also been reported by other authors. For instance, Oro and Martínez (1994) showed a *L. audouinii* colony breeding in the Ebro Delta (Spain) and wintering in the Senegambia region (West Africa).

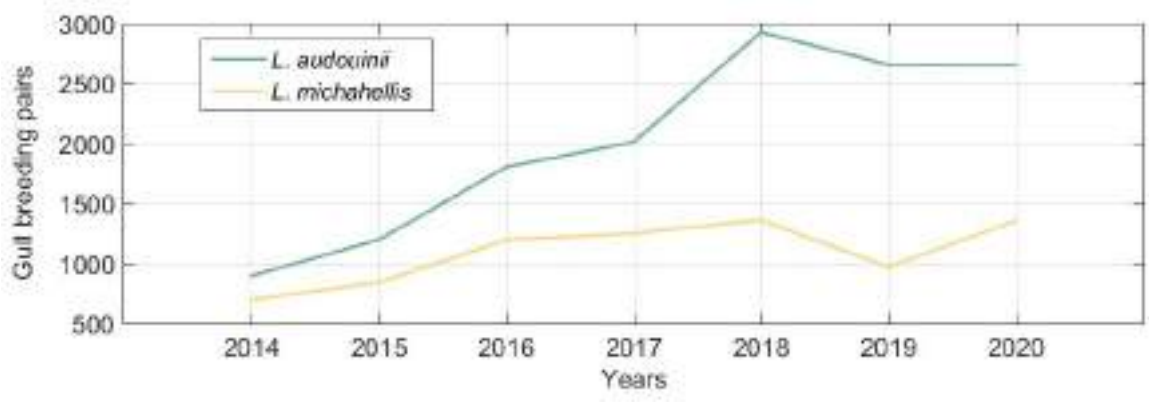

Figure 23 | Number of *L. michahellis* and *L. audouinii* breeding pairs in Barreta Island, from 2014 to 2020 (data shared by the University of Coimbra and SPEA).

8 | Data integration and analysis

8.1 Barrier island evolution

The longshore sediment transport towards the East, the jetty construction in the Faro-Olhão Inlet, and the Ancão Inlet relocation are natural and artificial factors causing the observed cross-shore growth trend in Barreta Island during the last 60 years (Kombiadou *et al*., 2019). This artificially enhanced growth suggests that progradation will still occur in some parts of the island allowing room for the development of new grey dunes. However, the progradation rates observed could be decelerated in some areas due to the rise in sea levels and derived erosion, an expected consequence linked to climate change. On the other hand, an ongoing or worsening process of the

vegetation disturbance in the central part of Barreta could set the conditions for the eventual shift of the dune state in those areas, from fixed to mobile. This eventual shift could pose serious consequences in the long-term, as grey dunes are fixed dunes, more or less colonized by plants and of extreme importance for the protection of the shoreline against the advances of the sea.

8.2 Dune degradation

The main direct factor causing the observed grey dune degradation in Barreta Island is, mostly, the gull populations settled in the the central part (both in the western and eastern DAs) and to a much minor extent the human action, namely trampling to acces the seaside and the back-barrier beaches.

8.2.1 Human interference

Examples highlighting the impacts of human occupation in the grey dune are shown in Figure 24. The easternmost area of the island experienced an ongoing development of human-related activities nearby the restaurant through the analysed years (only the 2008 and 2017 datasets are shown), which makes this area to always appear disturbed or partially disturbed as shown in all the correspondent index maps. For instance, the trampling paths located to the north of the restaurant are wider in 2008 than in 2017, thus the degree of degradation shown in the index maps changed from disturbed (light red) to partially disturbed (yellow) in those areas, respectively (Figure 24). However, in addition to the human-related disturbance, there are also vegetation shifts that influence the degradation index which are attributed to the natural vegetation seasonality and the quality of the images (e.g. colour, light conditions, exposure, shadows).

Additional evidence that corroborates the contribution of the human occupation to the dune disturbance can also be observed near the fishermen warehouses (Figure 25). The removal of the fishermen warehouses and related activities in the northern area of the island (end of 2014 or early 2015) caused the vegetation to re-grow in the following years, which led to a shift in the grey dune composition (sand cover was reduced) changing from disturbed or partially disturbed to optimal in some areas (see vegetation shifts from 2008 to the 2017 index maps in Figure 25). In this case, vegetation shifts in some regions are also attributed to vegetation seasonality and again with the differences in the quality of the datasets.

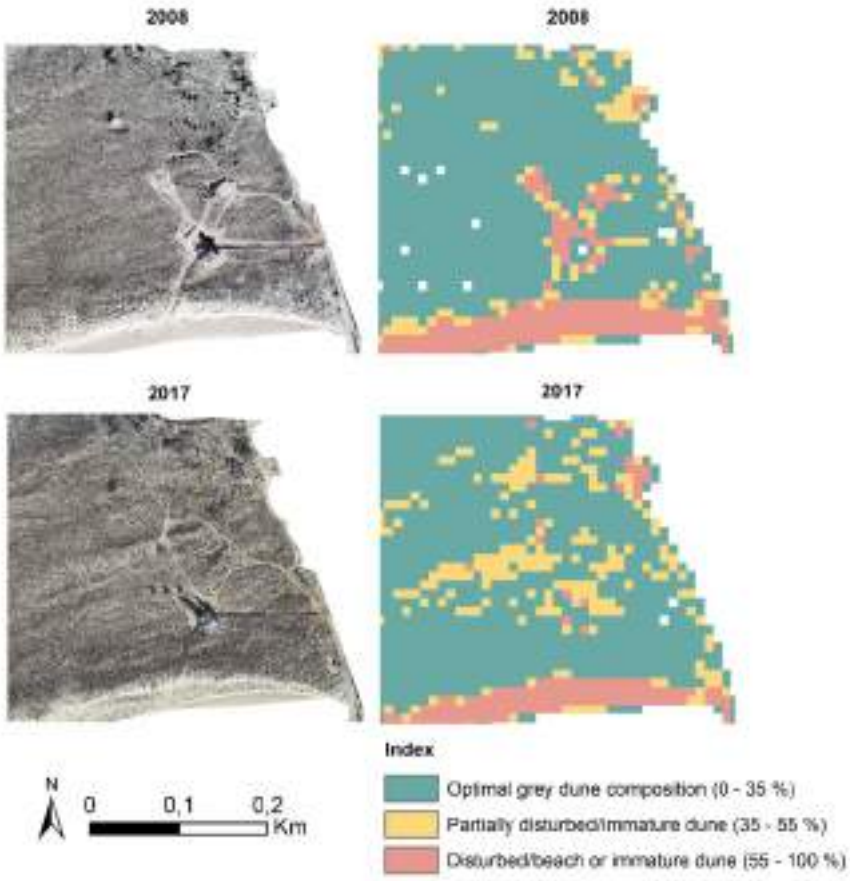

Figure 24 | Effects of the human occupation in the vegetation index in 2008 and 2017.

Despite the influence of seasonality and the image quality in the results, it is clear that the human-derived activities and occupation in Barreta Island induce changes in the composition of the grey dunes, contributing to both their recovery (warehouse removal) or degradation (trampling). Nevertheless, these seem to be quite located situations with a relatively small expression when compared to the overall island dimension.

8.2.2 Gull interference

Despite the local disturbance linked to human occupation, the gull populations seem to contribute for the large majority of the grey dune degradation in Barreta Island, causing the vegetation disturbance and degradation of large areas. The disturbance identified in the grey dunes (DAs) largely coincide with the distribution areas of Yellow-legged Gull and Audouin's Gull in the central part of Barreta, although *t*his species has a much smaller impact over the dune degradation than Yellow-legged Gull (see red circles corresponding to distribution areas of Yellow-legged Gullover the most disturbed vegetation areas in light red; Figure 26). This is mostly related not to differences in both populations size and/or density but to the migration of Audouin's Gull during the winter and the permanence during most of the year of Yellow-legged Gull (Matos *et al.*, 2018). This leads to problems in the areas occupied by *L. michahellis* as the disturbed dune vegetation is not able to recover during the non-breeding season.

Gull activities are often beneficial to flora, small fauna (Ólafsson 1982) and other organisms (such as bacteria and the invertebrate community that feeds on these) (Petersen *et al*., 2009) due to different behavioural reasons: transport of nutrients from the ocean onto land in the form of food remains and animal carcasses that they accumulate during nesting; and also regurgitation and defecation.

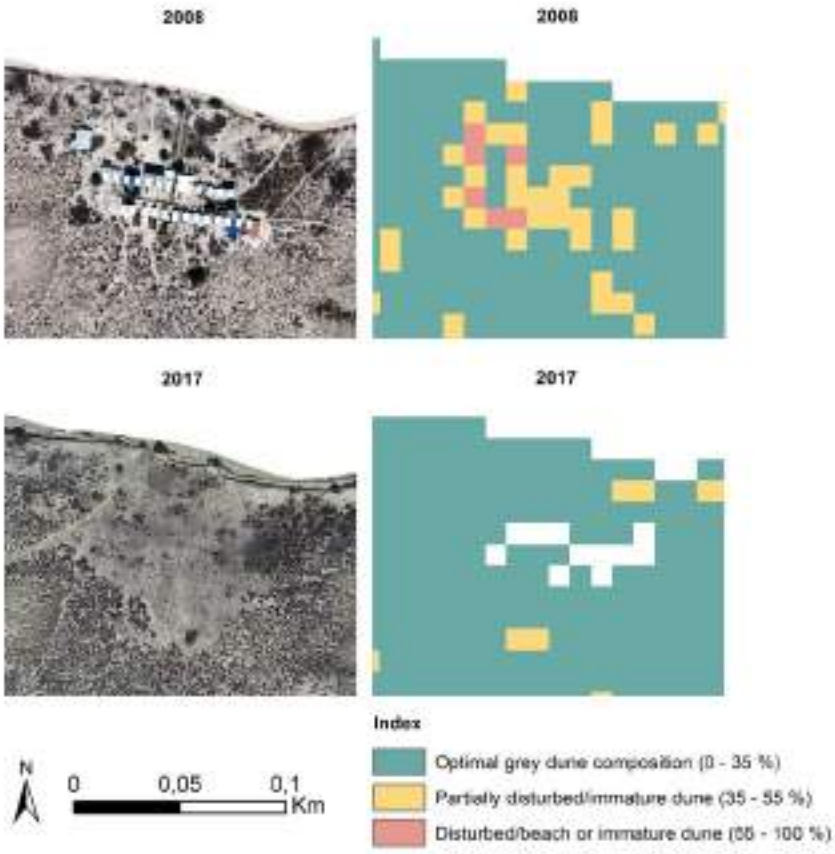

Figure 25 | Effects of the fishermen warehouses removal in the vegetation index (only the years 2008 and 2017 datasets and computed index maps are shown).

On the other hand, during the nesting period they can cause significant physical disturbance through burrowing as well as activities that directly damage plant tissues (e.g. trampling, uprooting and pulling leaves off plants) (Ellis *et al*., 2005). The negative implications linked to gull physical disturbance are further aggravated in Barreta Island in the areas occupied by Yellow-legged Gull. Similarly, nutrients from guano deposition that *a priori* are considered beneficial to plants can become highly concentrated and unfavourable to plants at high deposition rates (Sanchez-Piñeiro and Polis 2000), as the decomposition of guano in the soil often leads to an increased soil acidity (Ward 1961; Blakemore and Gibbs 1968). However, Gillham (1956) suggested the sea spray may confound this effect, and the combination of guano and sea spray can increase soil pH, mainly due to the effects of sea spray.

The effects that guano has on vegetation are not only dependent on deposition rates but also on precipitation and temperature. Investigations shown in Ellis *et al.* (2005) stated that in hot and dry climates, the nutrients from guano are either unavailable to plants, or at high deposition rates become highly concentrated and toxic to plants much more quickly than in temperate zones where higher rates of precipitation dilute high concentrations of guano. In addition, other studies on arid islands (Polis *et al*. 1997; Anderson and Polis 1999; Sanchez-Piñeiro and Polis 2000) showed that biomass and cover of annual plants increased dramatically on seabird islands in wet years. However, in dry years, the cover of plants was lower on all islands, but even lower on seabird roosting islands than islands withouth birds because high rates of soil evaporation combined with large amounts of guano created soil conditions that were harmful to plants (Sanchez-Piñeiro and Polis 2000). On the other hand, in cool and wet islands additional studies showed that biomass was greater in areas influenced by seabirds compared to areas without birds, except where densities of birds were extremely high (Ellis *et al*., 2005).

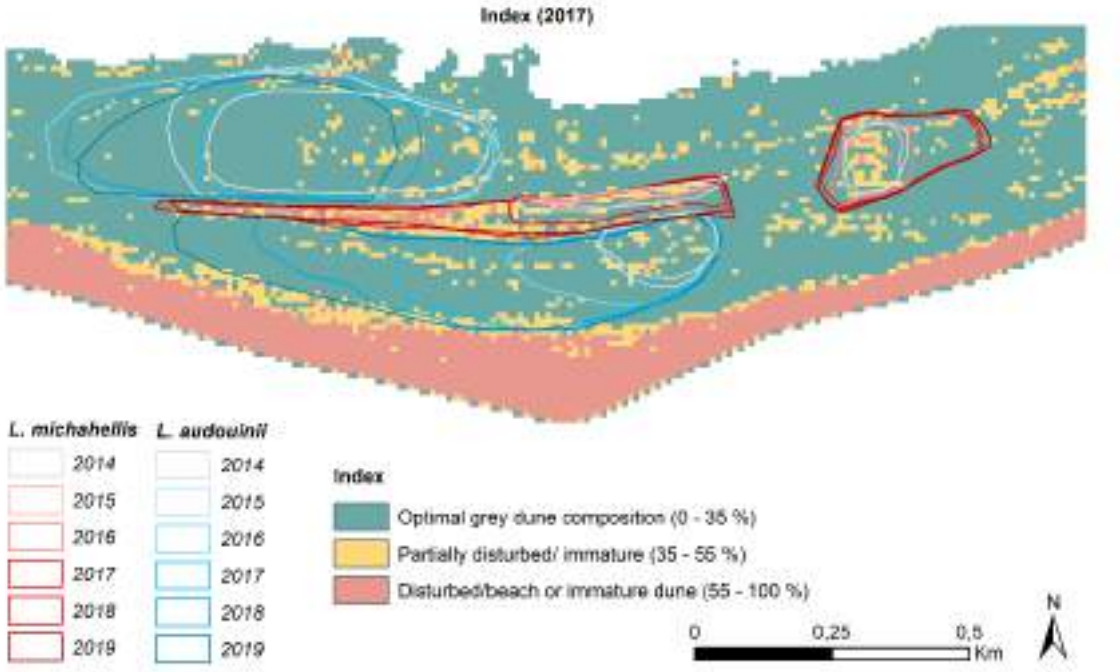

Figure 26 | Effects of the gull occupation in the 2017 vegetation index.

The importance of water for the vegetation cover and natural shift was actually observed in the disturbed areas in Barreta in May 2020, as there was a blooming of plants due to several rainfall episodes that occurred during that spring (Figure 27). This vegetation shift is a reflection of seasonal precipitation, and does not explain the plant degradation trend observed from 2014, which is mainly the result of an increase gull pressure. However, precipitation should be taken into account in case the aridity persists or intensifies due to climate change, as guano could increase its toxicity and lead to same or worse dune degradation.

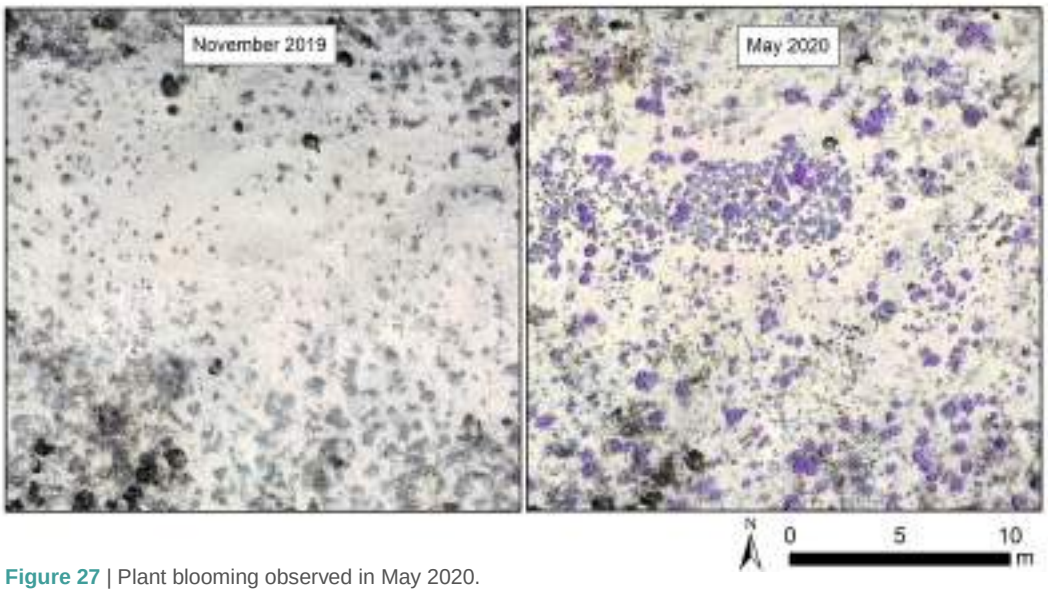

Figure 27 | Plant blooming observed in May 2020.

Besides, some studies have inferred that the organic matter derived from guano seems to decrease the water-retention capacity and moisture of the soil that seabirds occupy, thus impacting also the vegetation (Gillham, 1956). However, other works found no difference in soil moisture in colonies of burrowing procellarids and gulls (Mulder and Keall, 2001).

Another possible reason that could in part explain the different degree of disturbance between both gull species could be the different topography of both gull distribution areas in central area at Barreta and their proximity to the shore. Differences in the elevation of both gull distribution areas would in turn cause the water table depths to be further away in the higher areas (where the vegetation index shows the higher degree of disturbance) than in the lower ones, thus making it more difficult for the plants located in these higher regions to rely on it. The influence of the topography in the availability of water and the closer proximity to the shore could explain also the little effect that Yellow-legged Gull has in the lower westernmost part of the island, area occupied by this gull where no significant disturbance has been found other than the naturally higher cover of sand characteristic of inmature dunes and/or areas influenced by onshore aeolian sediment transport. This is singular, as the number of Yellow-legged Gull counted in the censuses in this western area is superior to those counted in the eastern DA at the central region of the island, which is located at higher elevation. In addition, the negative effect of an hyphothetical excess of guano deposition by *L. michahellis* in the soil and vegetation in the westernmost area of the island could be counteracted by the action of the sea spray, as stated before (Gillham, 1956b).

Taking into account all the previous, possible indirect factors contributing to the degradation of the grey dunes in Barreta Island could be the water availability for the plants, influenced by the topography and the precipitation as well as the amount of guano deposition and biomass generated by the gull populations.

9 | Conclusions

In this work the evolution of Barreta Island (and its geomorphological units) was investigated, the types and typical ranges of vegetation cover within the target grey dune habitat were identified, and an index to assess the evolution of its health state was built. To do so, remote-sensed data of different nature and resolution have been used from 1947 to 2020.

Barreta Island experienced a trend of artificially enhanced growth and marsh stability for the past 70 years due to natural longshore sediment transport directed towards the East, and past human actions such as the jetty construction in the Faro-Olhão Inlet and the Ancão Inlet relocation. Causes of disturbance in the vegetation cover of the grey dunes are mainly related to gull occupation (mostly due to the permanent trampling, physical disturbance to plants, and guano deposition caused by Yellow-legged Gull) and to a lesser extent to human occupation. However, further research would be needed in order to identify additional indirect factors contributing to degradation of the vegetation such as water availability linked to seasonal precipitation, soil moisture and/or changes in water table depths as a consequence of the island's variable topography.

Limitations inherent in the adopted approach that could have influenced the results are mainly related to the quality of the data used (datasets with different light conditions, exposure, presence of cloud shadows, etc.) and to natural seasonal changes in vegetation cover (datasets obtained in different seasons). To reduce the limitations derived from the image quality, virtual control areas in the datasets are going to be used in order to distinguish real vegetation cover changes from changes induced by different light conditions, exposure, etc. Moreover, upcoming UAS surveys during different seasons are going to help differentiate the natural vegetation seasonality changes (which may show natural plant degradation and/or recovery) from vegetation disturbance/recovery attributed to external factors such as the human and gull occupation. Despite the abovementioned limitations, two main disturbed areas have been clearly identified were conservation measures should be applied in order to minimise further degradation and to ensure the conservation of the grey dune habitat and associated species in Barreta Island.

ACKNOWLEDGMENTS

This work is funded by the project LIFE18 NAT/PT/000927 - LIFE Ilhas Barreira "Conserving the Barrier Islands in Algarve to protect priority species and habitats". Special thanks go to Animaris for the logistical support to conduct this work at Barreta Island, as well as to the University of Coimbra team and SPEA for sharing the gull census data. We also want to akckowledge Katerina Kombiadou and Xavier Herrero for sharing the results and figures of their respective works, as well as the DGT (Direção-Geral do Território) for providing the LiDAR-derived DTM and aerial photographs. We would also like to thank the different institutions that granted the permits needed to perform the UAS surveys in this area of Ria Formosa: ANAC (Autoridade Nacional da Aviação Civil), ANN (Autoridade Aeronáutica Nacional), ICNF (Instituto da Conservação da Natureza e das Florestas), and the Capitania Marítima do Porto de Faro.

REFERENCES

Anderson, W.B. & Polis, G.A. 1999. Nutrient fluxes from water to land: seabirds affect plant nutrient status on Gulf of California islands. Oecologia118: 324–332.

Andrade, C. 1990. O ambiente de barreira da Ria Formosa (Algarve, Portugal). University of Lisbon: Lisbon.

Almeida L.P., Ferreira, Ó., Vousdoukas, M.I. & Dodet, G. 2011. Historical variation and trends in storminess along the Portuguese South Coast. Natural Hazards and Earth System Sciences 11: 2407–2417.

Blakemore, L.C. & Gibbs, H.S. 1968. Effects of gannets on soil at Cape Kidnappers, Hawke's Bay. New Zealand Journal of Science. 11: 54–62.

Cohen, J. 1960. A coefficient of agreement for nominal scales. Educational and Psychological Measurements 20: 37-46.

Costa M., Silva, R. &Vitorino, J. 2001.Contribuição para o estudo do clima de agitação marítima na costa portuguesa. Proceedings of 2as Jornadas Portuguesas de Engenharia Costeira e Portuária, International Navigation Association PIANC, Sines, Portugal (in Portuguese)

Dias, J.A. & Neal, W.J. 1992. Sea cliff retreat in southern Portugal: profiles, processes, and problems. J Coast Res 8(3):641–654.

Ellis, J.C. 2005. Marine Birds on Land: A Review of Plant Biomass, Species Richness, and Community Composition in Seabird Colonies. Plant Ecology 181(2): 227-241.

Fleiss, J.L., Levin, B. & Paik, M.C., 2013. Statistical methods for rates and proportions. Wiley.

Gillham, M.E. 1956. Ecology of the Pembrokeshire Islands: V. Manuring by the colonial seabirds and mammals, with a note on seed distribution by gulls. Journal of Ecology 44: 429–454.

Herrero, X. 2018. Evaluation of coastal barrier constructive processes on Barreta. Vrije Universiteit: Amsterdam.

Herrero, X., Costas, S. & Kombiadou, K. 2020. Coastal ridge constructive processes at a multidecadal scale in Barreta Island (southern Portugal). Earth Surface Processes and Landforms 45: 411-423.

Jackson, D.W.T., Costas, S., González-Villanueva, R. & Cooper, A. 2019. A global 'greening' of coastal dunes: An integrated consequence of climate change? Global and Planetary Change 182: 103026.

Kombiadou, K., Matias, A., Ferreira, Ó., and Carrasco, A.R., Costas, S. & Plomaritis, H. 2019. Impacts of human interventions on the evolution of the Ria Formosa barrier island system (S. Portugal). Geomorphology 343: 129-144.

Matias, A., Ferreira, Ó., Vila-Concejo, A., Garcia, T. & Dias, J.A. 2008. Classification of washover dynamics in barrier islands. Geomorphology 97:655–674.

Matias, A., Ferreira, Ó., Vila-Concejo, A., Morris, B. & Dias, J. 2009a. Foreshore and hydrodynamic factors governing overwash. Journal of Coastal Research 56: 636–640.

Matias, A., Vila-Concejo, A., Ferreira, Ó., Morris, B. & Dias, J.A. 2009b. Sediment dynamics of barriers with frequent overwash. Journal of Coastal Research 25: 768–780.

Matos, D.M., Ramos, J.A., Calado, J.G., Ceia, F.R., Hey, J. & Paiva, V.H. 2018. How fishing intensity affects the spatial and thropic ecology of two gull species breeding in sympatry? ICES Journal of Marine Science 75 (6): 1949–1964.

Mulder, C.P.H. & Keall, S.N. 2001. Burrowing seabirds and reptiles: impacts on seeds, seedlings and soils in an island forest in New Zealand. Oecologia 127: 350–360.

Ólafsson, E. 1982. The status of the land-arthropod fauna on Surtsey, Iceland, in summer 1981. Surtsey Research Progress Reports IX: 68–72.

Oro, D. & Martínez, A. 1994. Migration and dispersal of Audouin's gull *Larus Audouinii* from the Ebro Delta colony. Ostrich-Journal of African Ornithology 65(2):225-230.

Petersen, A. 2009. Formation of a bird community on a new island, Surtsey, Iceland. Surtsey Research (2009) 12: 133–148.

Pacheco, A., Vila-Concejo, A., Ferreira, Ó. & Dias, J.A. 2008. Assessment of tidal inlet evolution and stability using sediment budget computations and hydraulic parameter analysis. Marine Geology 247:104–127.

Polis, G.A., Anderson, W.B. & Holt, R.D. 1997. Toward an integration of landscape and food web ecology: the dynamics of spatially subsidized food webs. Annual Review of Ecology and Systematics 28: 289–316.

IPMA, I. P. 2019. Website of the Portuguese Institute for Sea and Atmosphere I.P. URL: www.ipma.pt

Rusu, L., Pilar, P. & Guedes Soares, C. 2008. Hindcast of the wave conditions along the west Iberian coast. Coastal Engineering 55: 906-919.

Sanchez-Piñeiro, F. & Polis, G. A. 2000. Bottom-up dynamics of allochthonous input: direct and indirect effects of seabirds on islands. Ecology 81: 3117–3132.

Sen, P.K. 1968. Estimates of the regression coefficient based on Kendall's tau. Journal of American Statistical Association 63: 1379-1389.

Thieler, E.R., Himmelstoss, E.A., Zichichi, J.L. & Ergul, A. 2009. Digital Shoreline Analysis System (DSAS) version 4.0—An ArcGIS Extension for Calculating Shoreline Change. US Geological Survey Open-File Report. US Geological Survey: Reston, VA

Vila-Concejo, A., Matias, A., Ferreira, O., Duarte, C. & Dias, J. 2002. Recent evolution of the natural inlets of a barrier island system in southern Portugal. Journal of Coastal Research 36: 745–752.

Vila-Concejo, A., Matias, A., Pacheco, A., Ferreira, Ó. & Dias, J.A. 2006.Quantification of inlet-related hazards in barrier island systems. An example fro the Ria Formosa (Portugal). Continental Shelf Research 26: 1045-1060.

Ward, W.T. 1961. Soils of Stephens Island. New Zealand Journal of Science 4: 493–505.

ANNEXES

A – Percentace cover of Class 3 (sand) for each year in the whole Barreta Island and the western and eastern DAs

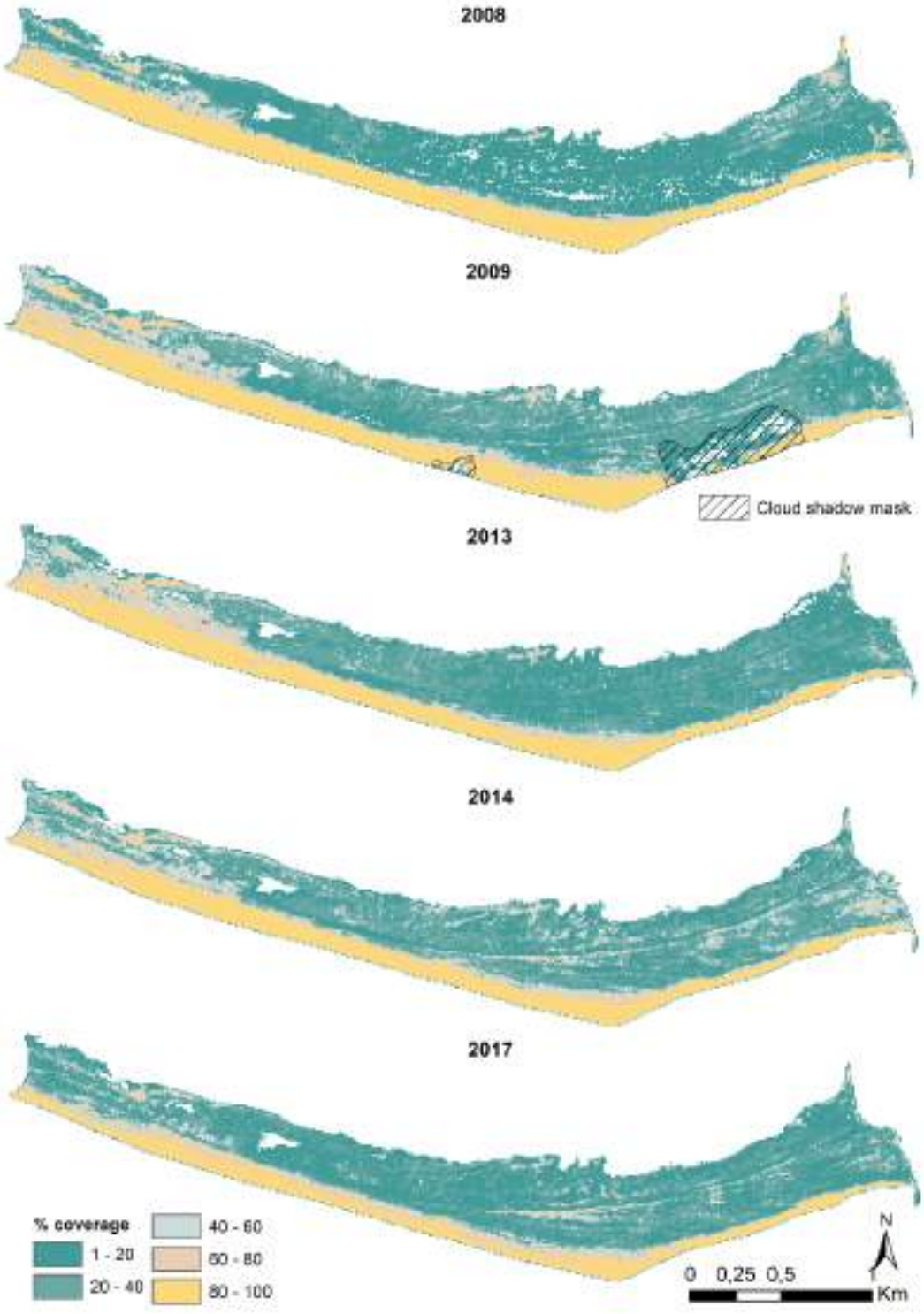

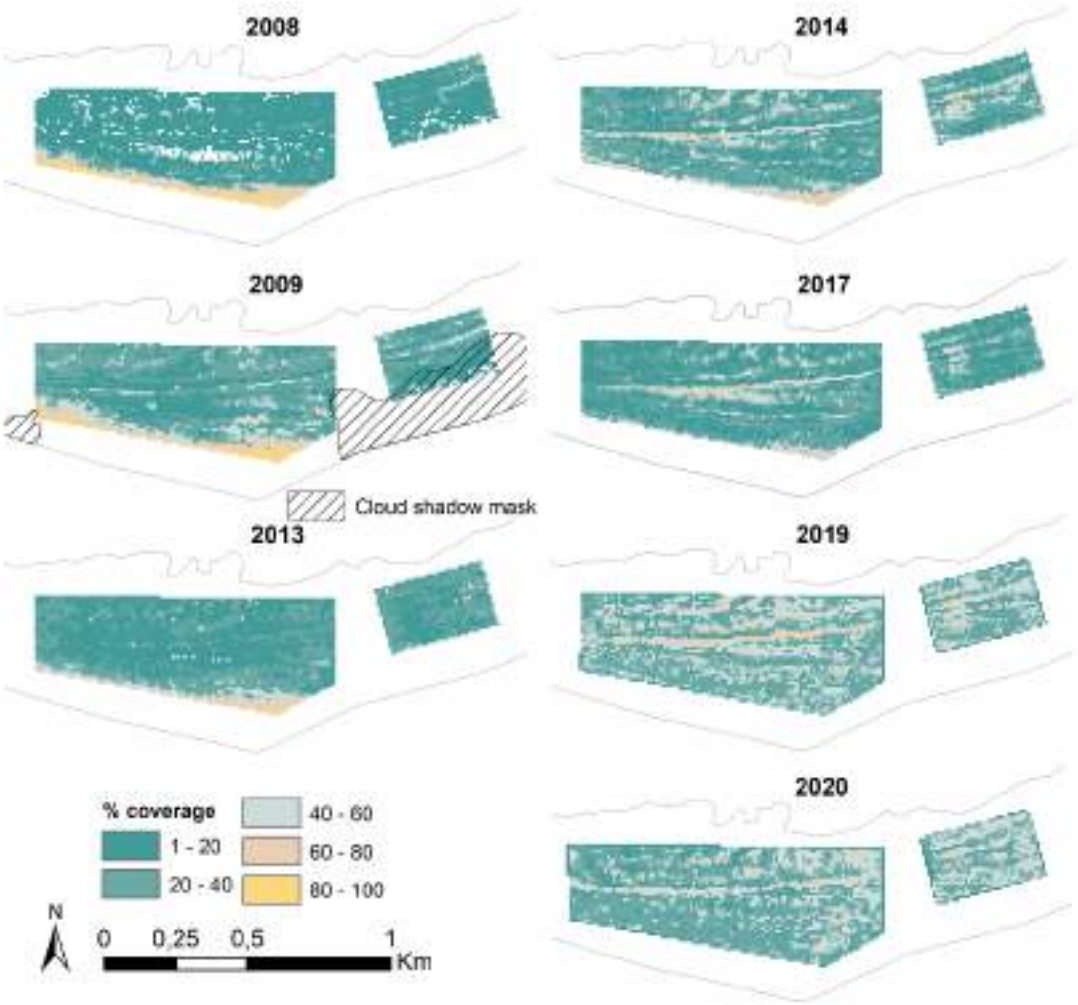
2008
2014
2009
2017
Cloud shadow mask
2013
2019
2020
% coverage
1 - 20
20 - 40
40 - 60
60 - 80
80 - 100
N
0
0,25
0,5
1
Km